Structural Design of Sea Gates against Tsunami Loads considering Ultimate Strength

POOKOTT ALANCHERY Amith Prasad

Master Thesis

presented in partial fulfillment
of the requirements for the double degree:
“Advanced Master in Naval Architecture” conferred by University of Liege
"Master of Sciences in Applied Mechanics, specialization in Hydrodynamics, Energetics and Propulsion” conferred by Ecole Centrale de Nantes

developed at West Pomeranian University of Technology, Szczecin
in the framework of the

“EMSHIP”
Erasmus Mundus Master Course
in “Integrated Advanced Ship Design”

Ref. 159652-1-2009-1-BE-ERA MUNDUS-EMMC

Supervisor:	Prof. Maciej Taczala, West Pomeranian University of Technology, Szczecin
Internship tutors:	Prof. Iijima Kazuhiro and Prof. Akira Tatsumi, Osaka University, Japan
Reviewer:	Prof. Rigo Philippe, University of Liege, Belgium

Szczecin, February 2019

This page is intentionally left blank.

DECLARATION OF AUTHORSHIP

I declare that this thesis and the work presented in it are my own and have been generated by me as the result of my own original research.

Where I have consulted the published work of others, this is always clearly attributed.

Where I have quoted from the work of others, the source is always given. With the exception of such quotations, this thesis is entirely my own work.

I have acknowledged all main sources of help.

Where the thesis is based on work done by myself jointly with others, I have made clear exactly what was done by others and what I have contributed myself.

This thesis contains no material that has been submitted previously, in whole or in part, for the award of any other academic degree or diploma.

I cede copyright of the thesis in favour of the West Pomeranian University of Technology, Szczecin

Date: *Signature*

This page is intentionally left blank.

ABSTRACT

Structural Design of Sea Gates against Tsunami Loads considering Ultimate Strength

By **POOKOTT ALANCHERY Amith Prasad**

The aftermath of Tohoku Tsunami (Japan, 2011), cost the country some major destruction to both life and property. In this context, the concept to deploy a steel water gate around the metropolitan areas that would protect the land against any future Tsunami that may occur was developed. The principle behind the action of the gate is the automatic erection of the structure that normally lies on seabed upon the action of Tsunami hydrodynamic lift and drag forces. Hence the gate has to have sufficient strength against the Tsunami loads that occurs once in tens of thousands years.

The Sea gate is already being designed and the functionality of the structure has been proved by performing a series of hydraulic tests on small scale models. Since the tsunami event is very rare and extreme, the design is made by using the so-called Level II methodology for reasonability (allows plastic deformation while keeping functionality), instead of Level I methodology (allows only elastic deformation).

The objective of this research is to check the structural behaviour of the sea gate against extreme hydrodynamic Tsunami loads and to evaluate the ultimate strength of the structure. For this purpose, a finite element mesh model of the innovative steel made gate structure has to be prepared based on the drawings using the pre/post FE processor MSC PATRAN. The meshed model will then be exported to the FE software MSC MARC for nonlinear finite element analysis. This time only static analysis will be performed and the reason for the non-necessity of the dynamic analysis will be proved during the course of the research.

Finally, the research objective has to be fulfilled, by showing the structural safety of the Sea Gate under the Tsunami loads with the return period of over thousand years.

This page is intentionally left blank.

Table of Contents

List of Figures

List of Tables

1. INTRODUCTION

A series of waves in a water body caused by the displacement of a large volume of water, generally in an ocean or a large lake is termed as a Tsunami or a tidal wave or a seismic sea wave. It is normally triggered by the factors like volcanic eruptions, earthquake, underwater explosions, landslides, glacier calving, meteorite explosions etc. The wavelength of the Tsunami waves is much larger when compared to the normal sea waves. Unlike the normal sea waves which appear as a breaking wave, tsunamis appear initially like a rapidly rising tide comprising of a series of waves, with their periods ranging from minutes to hours.

Japan is a country known for its record history of Tsunamis. The Great East Japan earthquake off the Pacific coast of Tohoku, 2011 with a magnitude of 9-9.1(Mw) initiated some influential tsunami waves that stretched elevations of up to 40.5 metres (133 ft.) in Miyako in Tōhoku's Iwate Prefecture and which travelled up to 10 km inland , in the Sendai area. The death counts recorded were around 15,896 along with destruction to nuclear power plants, roads, railways, buildings etc. It was declared as the costliest natural disaster in history with the estimated economic cost of US$235 billion by the World Bank.

Based on the studies conducted by the joint Tsunami survey teams under the main survey group, as an aftermath of the 2011 Tohoku Tsunami, many conclusions were implemented on the characteristics of the tsunami wave. The unrivalled scale and the low frequency of occurrence are believed to have led to the complex behaviour of the wave. The performance of the Tsunami counter measures available then, before the tsunami were evaluated based on the survey and other experiments numerical analyses. This actually paved the way for the understanding of the limitations of the countermeasures used till then and made the government think of new possible ideas/technologies that could be implemented in future for better protection.

1.1. Characteristics of Tohoku Tsunami, Japan 2011

1.1.1. Conjunct surveys of Tsunami damage

[1] Unlike the data available for earthquake related to ground vibration via large number of seismometers, for tsunami it is difficult to have similar kind of data collection. The only possible methods available are with the help of GPS buoys, Sea Bottom Pressure sensors and tide gauges. Hence it is a must to conduct efficient surveys post Tsunami to understand the calamity, it’s near shore effects as well as inland effects.

Moreover, to ensure proper collection of evidence over more than around 100 km range, before it washes away in time and due to rescue operations, a proper coordination between the

survey groups with the military support was maintained post 2011 Tsunami. Around 300 Japanese researchers and other international researchers comprised of the Tohoku Tsunami Joint Surveys Group (TTJS). Figure 1 shows a survey team in Kamaiti Iwashi prefecture, the survey which led to a conclusion of recording a tsunami height of 14.5m T.P, when the available Sea Wall Height is only 5.6 m T.P.

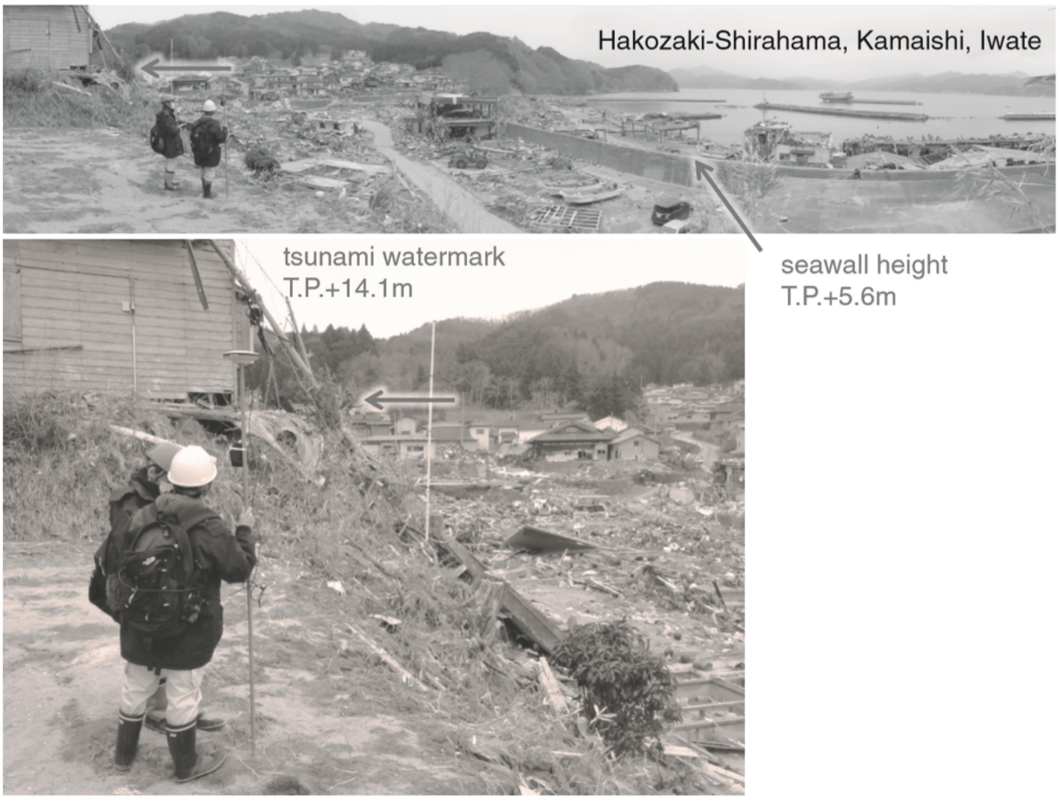

Figure 1 Tsunami water mark survey in Kamaishi, Iwate prefecture (April 11, 2011) [1]

1.1.2. Role of Sea Walls in Tsunami damage reduction

[1]Many concrete seawalls that were used as prevention against the Tsunami damage were either collapsed fully or partially. It was difficult to explain the contrasting characteristics shown by sea walls of different dimensions in an unexpected manner as a result of Tsunami. Figure 2 shows a partially collapsed concrete Sea Wall which was subjected to 2011 Tsunami, at Kojira-hama, Touni, Iwate prefecture.

Figure 2 Partially Damaged Sea Wall (Iwate Prefecture: June 9, 2011) [1]

Studies were conducted to explain the contrasting behaviour of Sea Walls in different areas. Experts concluded that the factors like the availability of the gravel fill on the slope of landside as well as the partitioning walls present inside the sea walls made a major impact on the structural integrity of the structure. The presence of the above two factors made the wall more effective against the damage. Figure 3 shows a survived sea wall in Fukushima that was having the mentioned benefits.

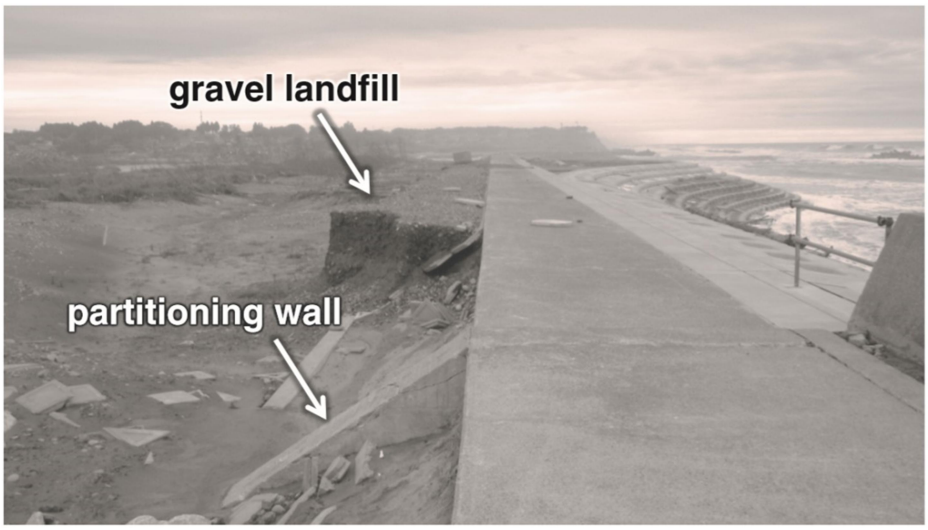

Figure 3 Survived Seawall in Fukushima prefecture (June 20, 2012) [1]

1.1.3. Tsunami Propagation-Numerical Stimulation

[1]When the Tsunami source is known, linear long wave equation is used to numerically simulate the Tsunami propagation. The equation is as follows,

$$\frac{\partial \eta}{\partial t} + \frac{1}{R\cos\varphi}\left[\frac{\partial M}{\partial \lambda} + \frac{\partial}{\partial \varphi}(N\cos\varphi)\right] = 0 \qquad [1]$$

$$\frac{\partial M}{\partial t} + \frac{1}{R\cos\varphi} gh\frac{\partial \eta}{\partial \lambda} = 0 \qquad [2]$$

$$\frac{\partial N}{\partial t} + \frac{1}{R} gh\frac{\partial \eta}{\partial \varphi} = 0 \qquad [3]$$

R is the radius of the earth; λ is the longitude; φ is the latitude; η is the water surface elevation; h is the water depth & g is accelaration due to gravity

1.2. Steel Gates against Tsunami

1.2.1. The concept

As a result of the aftermath of the 2011 Tsunami, the government decided to implement new techniques/ideas based on research to minimalize the damage on lives and cities caused by any Tsunami disasters in future. Detailed studies proved that building sea gates from shore line at some distance inside shallow water would reduce the run up height of the Tsunami waves.

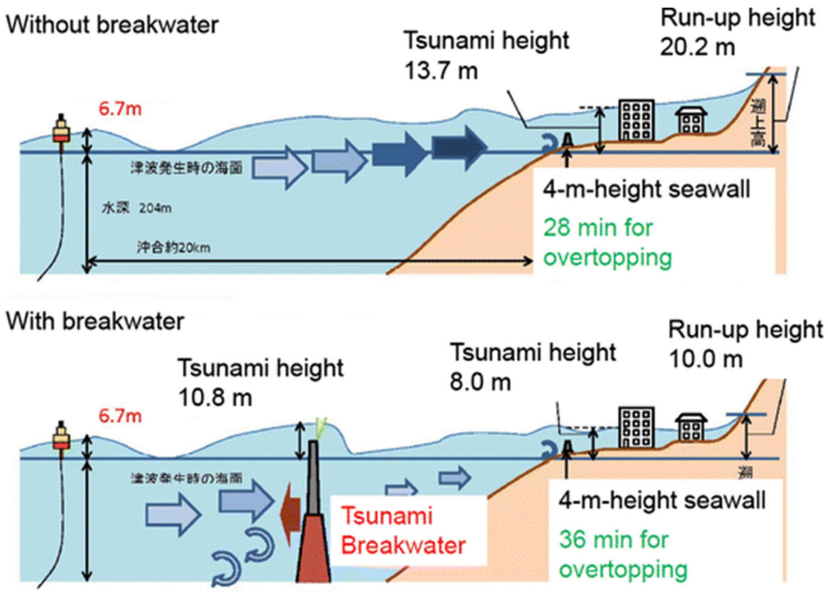

Figure 4 Tsunami break water and run up height of wave [2]

It was on this context the idea of implementing Sea Gates on the shallow waters near the metropolitan cities raised, which would stand up and act as a barrier against the Tsunami to mitigate the damage on land by decreasing the momentum of the waves. It can never stop the Tsunami flow totally, however the impact of the waves are reduced while crossing the gates. A research is being undergoing on the same and a water gate has been designed by some research institutions and other industries for this purpose.

The Hydroplane Tsunami Barrier is a kind of the movable breakwater. The main body is fixed to the pedestal by special rubber belts, and it rises by hydraulic force due to tsunami and storm surge. The effectiveness of this breakwater for tsunami countermeasures is indicated through experiments of response characteristics for hydraulic force, wave force acting on the main body and the damping effect for a wave height. Figure 4, 5 & 6 are the pictorial representations of the behaviour of the Sea Gates.

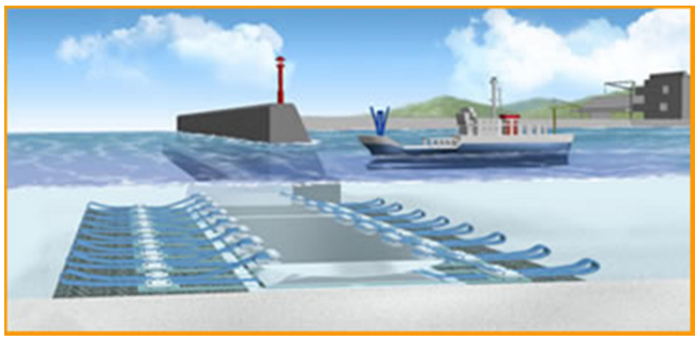

Figure 5 Sea gate in the lay down position

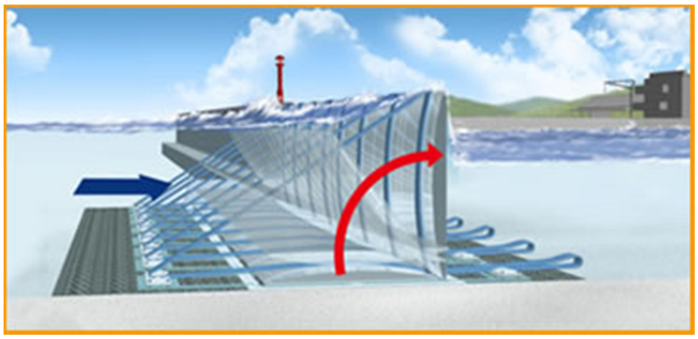

Figure 6 Sea Gate erection under the influence of Tsunami

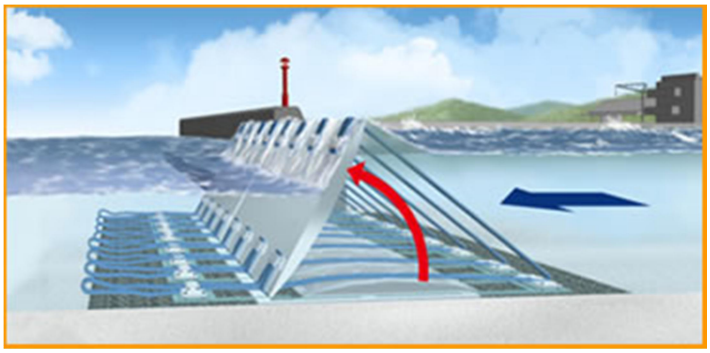

Figure 7 Sea Gate erection upon drawback action of Tsunami

1.2.2. Design Philosophy

The possible types of Tsunami waves that can hit the japan coasts are classified as Level I and Level II Tsunamis based on the severity and the possibilities of occurrence. Level I Tsunamis are comparatively smaller than Level II and the chances of occurrence for these are once in 100 years. Level II Tsunami on the other hand is more destructive with possibility of occurrence in every 1000 years. The design philosophy for the sea gate structure is different for L1 and L2 type of Tsunamis. Table 1 shows the idea behind the design philosophy of the structure [9].

Table 1 Design philosophy

Tsunami Type	Determination	Idea
Level I	Frequent Tsunami with return period of the order 100 years	1.Protect human lives, cities etc.
		2.Maintain whole structure of breakwater
Level II	Possible Tsunami with the return period of the order over 1000 years	1. Protect human lives.
		2. Minimise destruction of cities & economy.
		3. Maintain partial structure of the breakwater as possible.

1.2.3. Organizations involved in the research

Since the concept of Sea gates are new, many organizations are involved with the research and development of the project. Below schematic representation shows the member organizations involved. Osaka University, Japan is responsible for the structural performance analysis of the Seagate.

- ***Marsima Aqua System Corporation***: Design & Construction of the Tsunami Gate
- ***New Jec Inc.:*** Study on Tsunami waves and its characteristics
- ***Kyoto University:*** Hydraulic tests of the Sea Gate models
- ***Osaka Institute of Technology:*** Research & Development
- ***Port & Airport Research Institute:*** Research & Development
- ***Osaka University:*** Structural analysis of the design
- ***Mirai Construction Ltd.:*** Installation of the Sea Gate on site

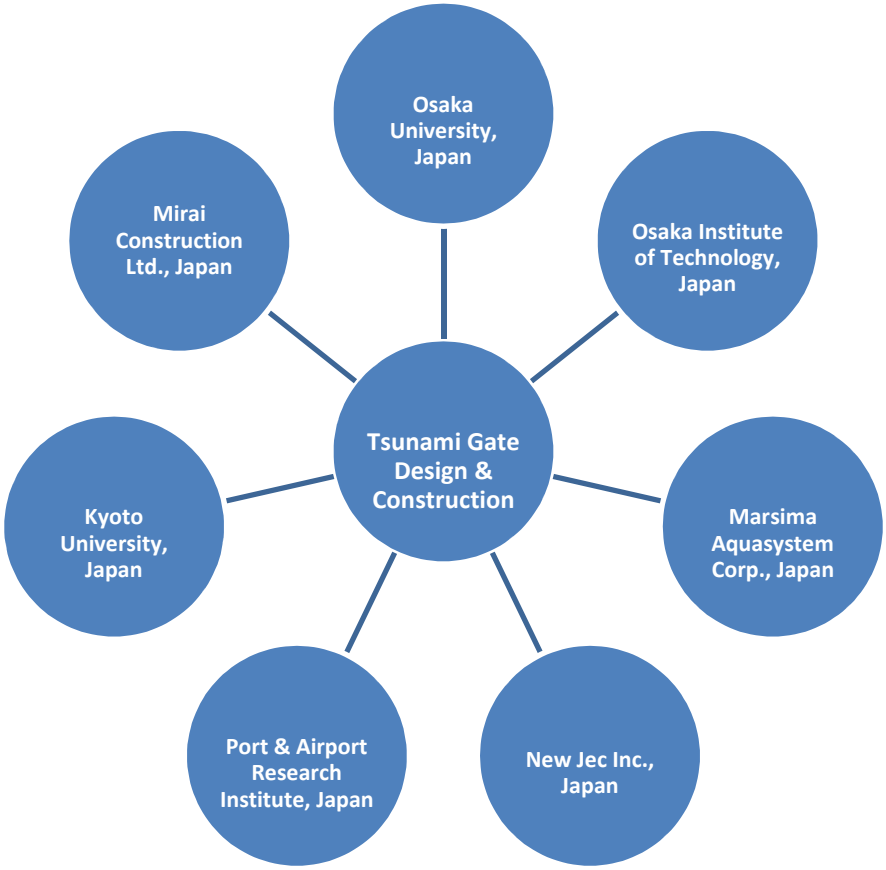

Figure 8 Organisations involved in the research

Figure 9 Prototype of the Sea Gate being constructed at MASC, Japan

1.2.4. Study conducted at the Kyoto University, Japan

[3] Prof. Ryoukei Azuma of Kyoto University, along with his team studied the functionality of the Hydroplane Tsunami barrier using two different models, i.e. 10cm high model and a comparatively large 43cm high model. The latter case experiment & results are studied here.

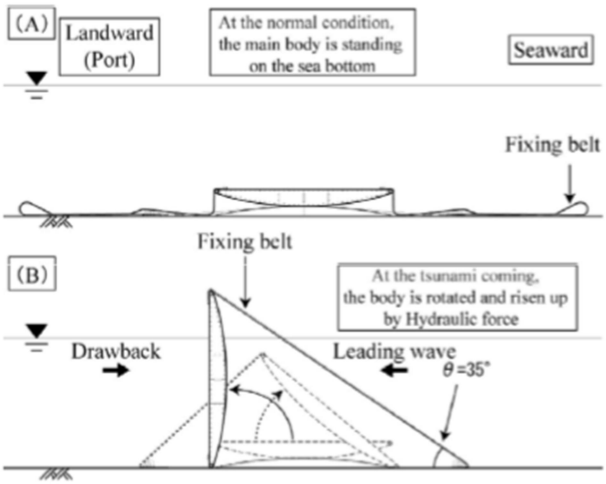

Figure 10 Barrier setup [3]

Figure 10 Cross sectional representation of the barrier at normal time (A) & at Tsunami (B)

The model is subjected to experiment in the Tsunami flume available at the Kyoto University, Japan. Two types of Tsunami waves, short tsunami waves generated by pistons and long tsunami wave generated by jet pumps are used in the experiment. Different cases are studied and recorded.

Table 2 Tsunami flume dimensions

Sl No.	Tsunami Flume Dimensions(m)	
1	Length	44
2	Width	4
3	Height	2
4	Water Depth	0.475

The below diagrams show the arrangement of the model inside the flume. The barrier is mounted on a mound which is 15cm high. Hence it can be seen that upon erection, 10.5cm of the barrier comes out of water.

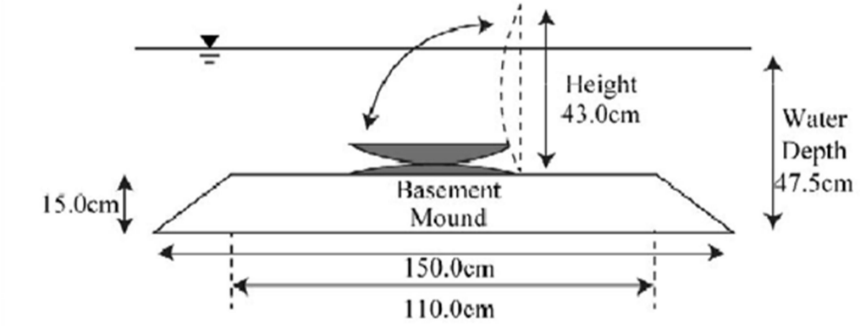

Figure 11 Model mounting set up [3]

Piston paddles to produce the short tsunami waves and jet pump outlets for the generation of the long tsunami waves are at a distance of 11.7 m from the basement mount. Also on both sides of the barrier electromagnetic anemometers and wave height meters are installed. The fixing belt of the barrier is not shown in these representations.

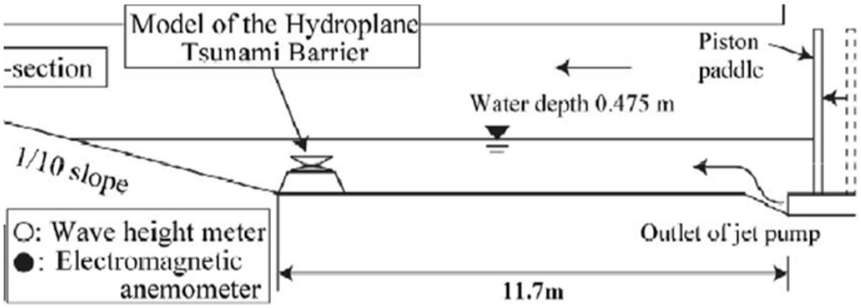

Figure 12 Side view, Tsunami flume setup [3]

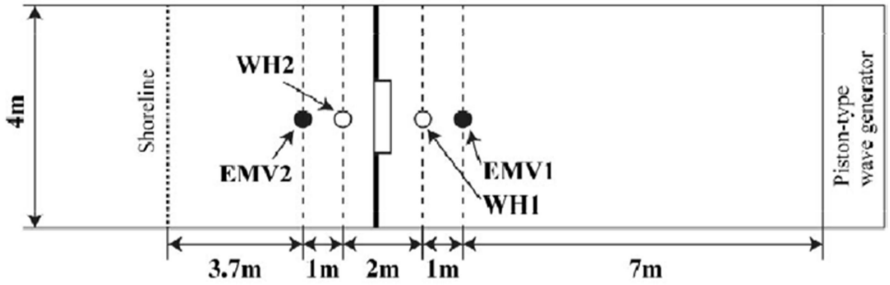

Figure 13 Plan view, Tsunami flume setup [3]

For the short tsunami waves, different wave height cases are generated and the behaviour of the barrier is noted. For the long tsunami waves different cases are generated by varying the pump discharge and the same procesure is carried out. Given below are the extract of the data & observations that were used and recorded in the course of the experiment.

Table 3 Short Tsunami wave characteristics generated and after barrier influence

Case	Wave Height(cm)	Max. water level variation(cm)		Max. velocity(cm/s)		Max. Tension(N)	Barrier erection
		Out	In	Out	In		
SW005	1.1	1.0	0.9	4.6	4.3	-	No
SW010	2.2	2.3	2.3	11.1	9.9	-	No
SW025	5.4	6.0	5.7	23.7	23.1	-	No
SW050	10.8	11.7	11.0	42.8	41.8	636.0	Yes
SW075	16.1	16.4	15.6	58.5	53.0	2261.0	Yes
SW100	21.5	21.8	19.4	76.1	63.9	3013.0	Yes

Table 4 Long Tsunami wave characteristics generated and after barrier influence

Case	Pump Discharge(m3/s)	Max. water level variation(cm)		Max. velocity(cm/s)		Max. Tension(N)	Barrier erection
		Out	In	Out	In		
FL005	0.05	0.5	0.4	5	2.5	-	No
FL010	0.1	1.3	1.3	5	2.9	-	No
FL030	0.3	7.9	4.3	16.3	14.5	177.0	Yes
FL050	0.5	14.2	5.2	27.2	21.5	360.0	Yes
FL070	0.7	20.0	7.2	37.7	27.5	683.0	Yes

It is clear from the tables above that the barrier does help in the decrement effect of both the wave height and the wave velocity. But the following points were to be noted

- The reduction effect on long period wave is larger when compared to the reduction effect in short period wave
- Also for both cases the reduction effect of the velocity is more than the damping effect of wave height
- The maximum tension recorded in the short wave case is much larger than the long wave case

Below graphs shows the maximum tension in belt case for both short and long perod waves.

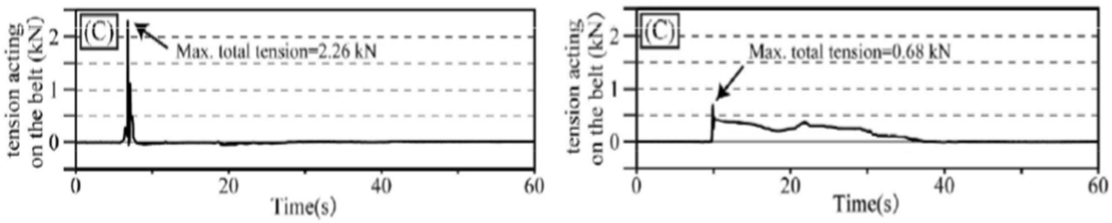

Figure 14 Time series data of tension acting on the belt [3]

It is noticed that the maximum tension in short wave is 2.26KN where as in long wave it is 0.68KN. For the short period waves the impact force at rising up and the wave force of maximum height wave acts simultaneously. In the case of long period waves the impact force at rising up is followed by the maximum height wave force after some time. This time delay explains the variation of the maximum belt force between both cases.

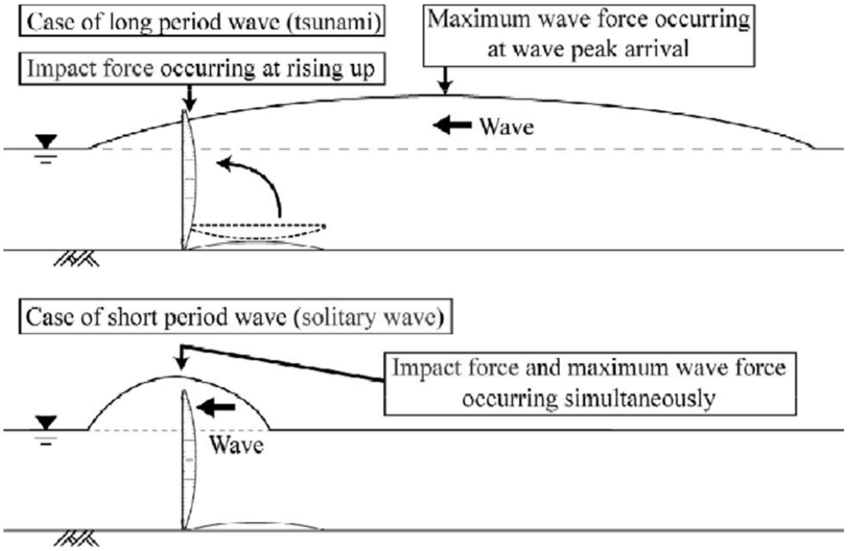

Figure 15 Difference in approach of both type of waves [3]

1.3. Areas of implementation

The government of Japan is planning to implement/install similar structures in various prefactures throughout the country. The most recent contract details shows the following prefactures, including Hyogo, Mie Town and Kochi and their corresponding ports , being sanctioned for the Sea Gate installation.

This report deals with the structural analysis of the Sea gate structure planned for the two locations(highlighted in the map below) at the Nukushima island port, Hyogo prefacture. Highlighted areas in Figure 16 are the two sites for the installation of the Sea gate structure.

Figure 16 Nushima Island Port, Hyogo prefacture [4]

1.4. Aim and Research methodology

The aim of this thesis work is to analyse the structural behaviour of the Sea Gate when subjected to L1/L2 type of Tsunami loads followed by the ultimate strength analysis when subjected to extreme Tsunami loads. The structure will be verified by using nonlinear static finite element analysis. The performance of the structure when subjected to such loads should meet the design philosophy.

Once the model is ready, the non-necessity of the dynamic analysis is to be proved. This is done by performing the Eigen value analysis on the model using the FEA solver once the model is ready, and showing that the natural frequency/period of the structure is in no range of the frequency/time period of the impact load of the Tsunami waves (converted large scale values from the model experiments).

Following steps are being carried out for the investigation

- Modelling & Meshing of the structure considering a symmetric section from the available drawings in MSC Patran

  Note: The model is developed from scratch as surfaces, in order to get a proper mesh; keeping in mind the intersection part between the stiffeners/stringer and the walls. Also an aspect ratio of 1 is tried to maintain for almost every element.
- Performing the Eigen value analysis of the structure in MSC MARC after importing the file generated in MSC Patran
- Extracting the frequency/time period of the impulse wave(model) from the results of experiments available and converting it to real scale
- Comparing the results to prove the non-necessity of the Dynamic Analysis
- Performing the Non Linear Progressive static analysis on the section using FEA solver MSC MARC against L1/L2 Tsunami loads
- Evaluating the Ultimate strength of the structure when subjected to extreme Tsunami loads

1.5. Methodology brief

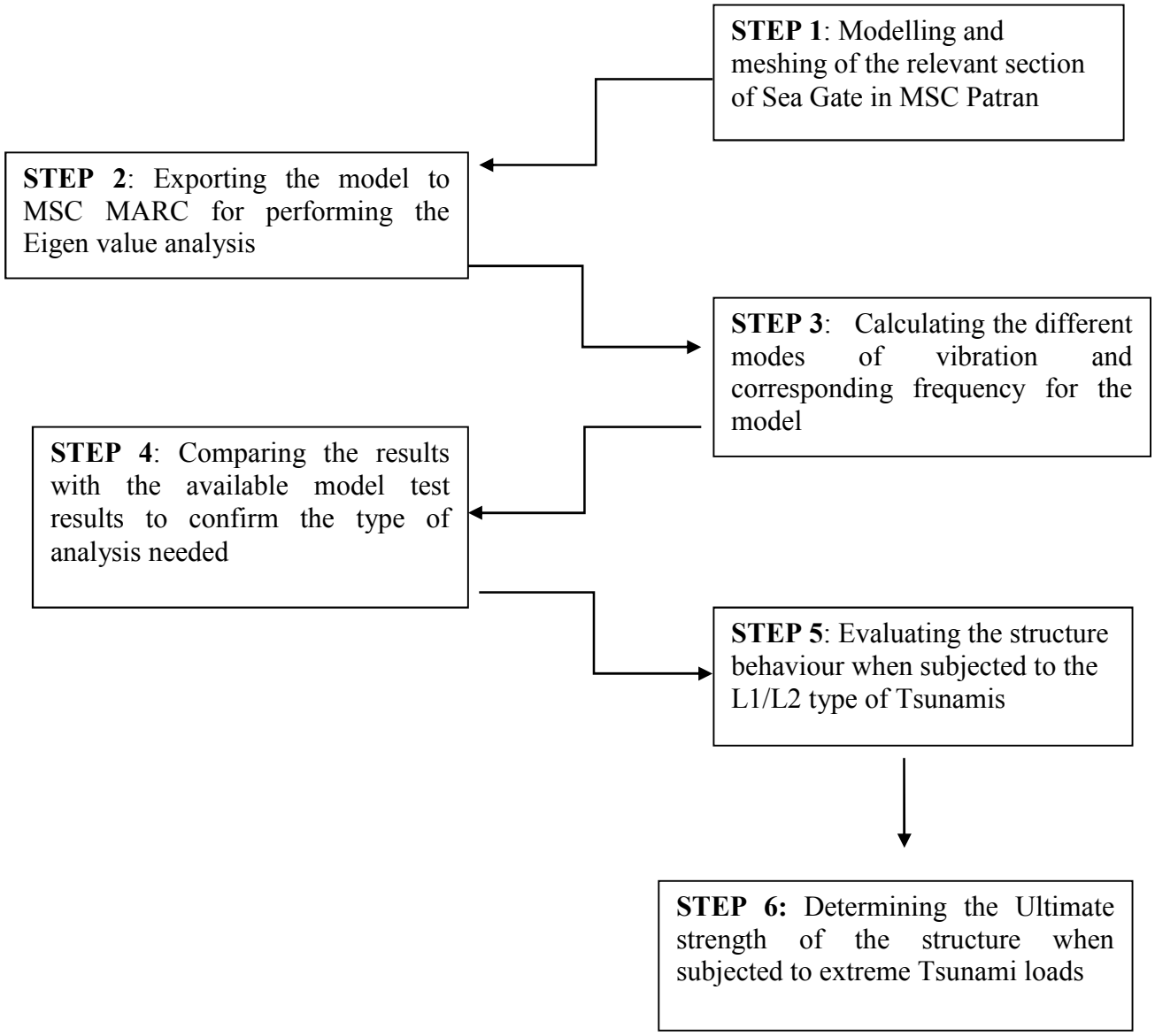

Methodology brief

The different steps involved as part of the methodology are shown above.

2. STRUCTURE UNDER INVESTIGATION

The structure under research for this thesis study is a vertical wall of height 10.33m that will be used as a counter measure for large Tsunamis that may be devastating in the future. The steel used for the structure is of grade SM 400 and the material for the belt associated with the structure is NN-450 S-S. The sites in which this structure is planned to install are mentioned in section 1.3.

2.1 Data available

The structure of width 20m and height 10.33m is planned to be installed at the site along with identical structures in the port openings depending on the criticality of the area.

The structural design has been carried out by Marsima Aqua System Corp., Japan. Below figures show the structural configurations of the same.

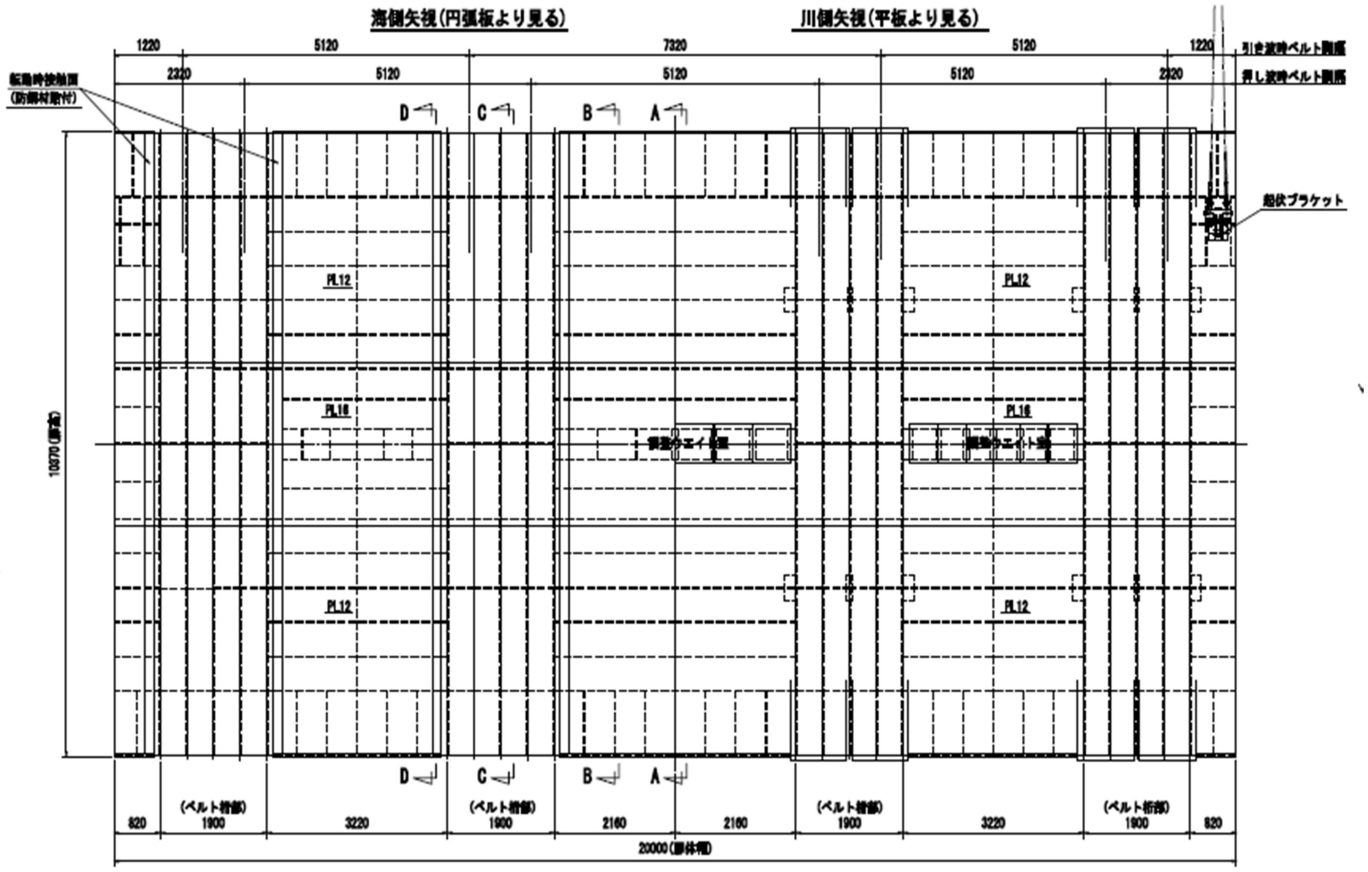

Figure 17 Front view of the Sea Gate

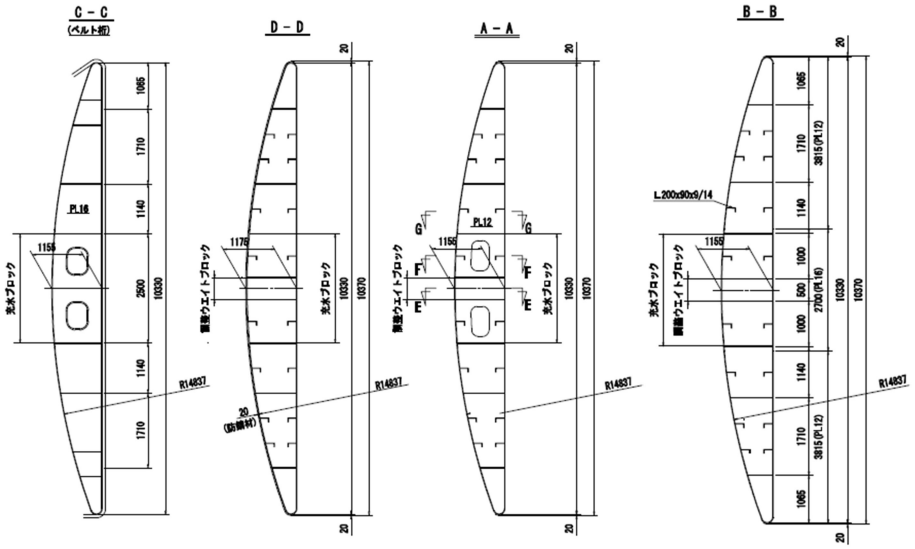

Figure 18 Section views (side) of the structure

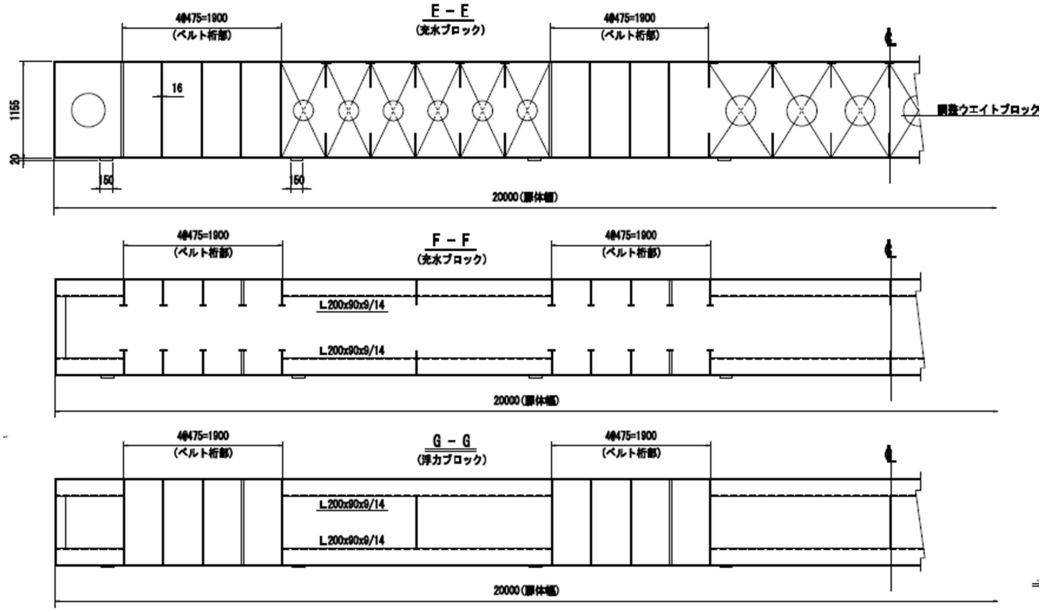

Figure 19 Section view (top)

2.2 Structural Configuration

A relevant section is considered within the structure, which in effect acts as a symmetric section when the structures are arranged together on site. The section is 5.67 m in width with same height as the original structure. Figure 21 shows the symmetric section which was considered for the analysis along with the structural configuration.

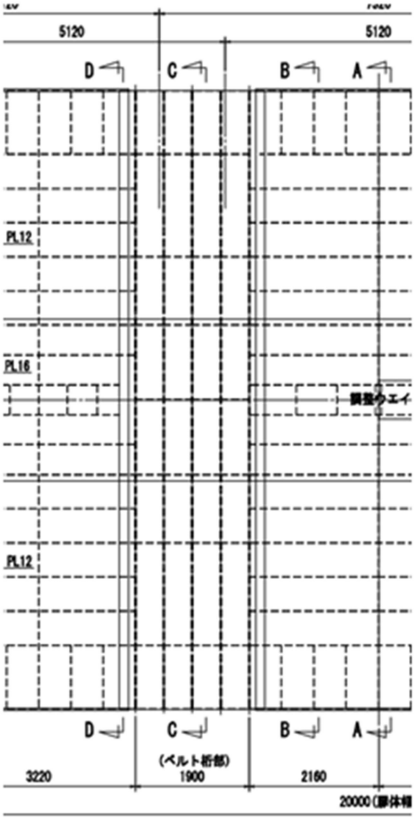

Part	Dimension/Reach(mm)	Qty
Curved Plate-Top	5670*3815*12	1
Curved Plate-Middle	5670*2700*16	1
Curved Plate-Bottom	5670*3815*12	1
Base Plate-Top	5670*3815*12	1
Base Plate-Middle	5670*2700*16	1
Base Plate-Bottom	5670*3815*12	1
Side Plate_Vertical	10330*1155(Max)*16	2
Strength Plate_Vertical	10330*1155(Max)*16	5
Strength Plate_Horizontal	1900*1155*12	1
Strength Plate_Horizontal	1610*1152*12	2
Strength Plate_Horizontal	2160*1152*12	2
Strength Plate_Horizontal	5670*1102*12	2
Strength Plate_Horizontal	5670*961*12	2
Strength Plate_Horizontal	5670*577*12	2
Stiffeners	1610*(200*9/90*14)	16
Stiffeners	2160*(200*9/90*14)	16
Top Plate	5670*226*12	1
Bottom Plate	5670*226*12	1

Figure 20 Symmetric section considered with the structural configuration

3. STRENGTH ANALYSIS BY FEM: THEORETICAL ASPECTS

3.1 Background

[5] In the field of engineering and science, many physical phenomena could be explained by using the partial differential equations. But in general for arbitrary shapes it is almost impossible to solve these equations using the normal analytical formulas. In this context, the numerical approach called Finite Element Method could be used to solve these partial differential equations approximately. In general FEM is a tool used to solve different engineering challenges like stress analysis, fluid flow, electromagnetics and heat transfer using computer simulation.

The basic FEM concept is to divide the structure into finite parts generally termed as elements which are connected by nodes. The elements and nodes together are called mesh and the process of creating a mesh is termed as mesh generation. The Finite Element method delivers an efficient approach by which the solution is attained using the computer simulation. A system of linear equation is solved for attaining the solution in case of linear problems. In this case the number of unknowns is equal to the number of nodes. Thousands of nodes are

needed for obtaining a considerably valid solution; hence computers are inevitable for solving these equations.

The majority of finite element analyses used in engineering design these days are still linear finite element analyses. While dealing with heat conduction problems, the linearity can only be applied when the heat conductance is independent of the temperature whereas for stress analysis linearity can be applied when the displacements are small and the material behaviour remains linear elastic. Nonlinear elastic analysis are performed for the simulation of extreme loads such as drop tests of electronic devices, crash loads etc.

The Finite element method was implemented in the 1950's for the aerospace industry. The then major companies involved in the development and implementation of the FEM process were Boeing and Bell Aerospace in the United States and Rolls Royce in the United Kingdom. In 1956 a paper was published by R.W Clough, M.J Turner, L.J Topp and H.C Martin which gave some major ideas in this field. Initially the FEM concept was looked upon sceptically and many journals refused to publish papers on this. But by the late 1960's many mathematicians got interested in the concept of FEM as they came across the fact that the finite element method converge to the apt solution of the partial differential equation for linear problems. It was also noted that, as the number of elements were increased the solution gets even well refined.

The first Finite Element program was developed by E Wilson in the early 1960's. The program which was limited to two dimensional stress analyses back then, later on got developed by several research institutions and laboratories which paved the way for gaining the trust in the method eventually. Later in 1965 a research project was initiated to develop a general Finite Element Program which was funded by NASA and was led by Dick MacNeal. This program which was later on named as NASTRAN had wide range of capabilities to perform operations like two & three dimensional stress analysis for beam and shell elements and also complex structures, vibration analysis and time dependent dynamic load response.

During this period, John Swanson of Westinghouse Electric Corp. developed a finite element program to analyse the nuclear reactors. In 1969, he marketed the software as ANSYS which in no time gained wide acceptance in the industry. The program had both linear and nonlinear capabilities for solving problems. LS Dyna is another nonlinear software package which evolved in more recent era. It was developed by John Hallquist at the Livermore National University initially. In the beginning the program had only dynamic capabilities for nonlinear cases and was used to solve sheet metal forming, prototype simulations such as drop tests and crash worthiness.

A company named HKS, cofounded in 1978 developed the program ABAQUS which initially focussed on nonlinear applications, but soon got updated with linear capability.

These days the possibilities of a wide range of analysis capabilities in one single software makes it easy to find solutions for complex real-life problems. Following are the basic five steps involved within a finite element method.

- Pre-processing : Segmenting the problem domain into finite elements
- Element formulation : Formulating the equations for elements
- Assembly : Deriving the equations for the entire system from the individual element equations
- Solving the equations
- Post processing : Shaping the quantities of interest such as stresses and strains and visualising the results

3.2 Understanding Nonlinearity

[6] Finite element analysis (FEA) was initially regarded only as an analyst's tool, whereas over the last decade it entered the practical world of design engineering. Now a days CAD software comes with built in FEA capabilities and for everyday design tool, FEA is being used by the design engineers in support of the product design process. Until recently, almost all FEA functions carried out by design engineers were limited to linear analysis. For most difficulties encountered by design engineers, such linear analysis gives a tolerable approximation of real life characteristics. Nevertheless, sometimes more exciting difficulties arise, difficulties that call for modern nonlinear approach.

Because of the long solution time and complex problem formulation, previously engineers were sceptic regarding the use of nonlinear analysis. The trend has shifted enormously in recent past as the nonlinear FEA software bridges with CAD and has become much more user friendly. Moreover the advanced solution algorithms and highly advanced desktop computers have reduced the solution time. FEA was recognised as a valuable design tool by the engineers a decade ago and recently a greater understanding of the nonlinear approach has opened the window that brought into light the benefits that the nonlinear FEA brings to the design process.

3.3 Disparities between linear and nonlinear analyses

The fundamental divergences between the linear and nonlinear analysis could be explained using stiffness. Stiffness can be termed as a property of a single part or an assembly that describes the structural response in terms of displacements when subjected to external loads. Stiffness of a material is affected by

- Shape : Stiffness is different between an I beam and a channel section

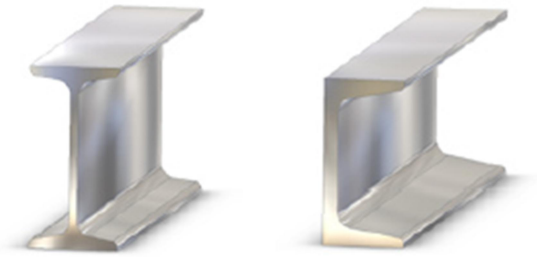

Figure 21 I beam and channel section with distinct stiffness [6]

- Material : A steel beam is more stiff than a similar shaped aluminium beam

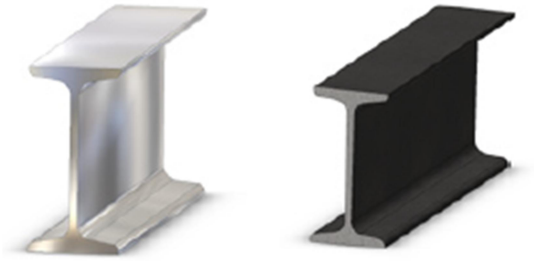

Figure 22 Varying stiffness for same section built in steel and aluminium [6]

- Support : A beam acting as a cantilever is less stiff than a beam supported at both ends

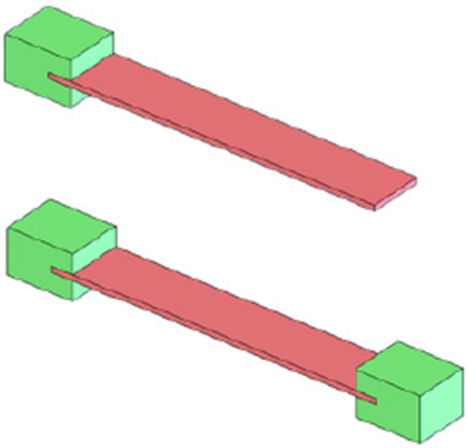

Figure 23 Stiffness dependency on support [6]

Due to one or more factors listed above, the stiffness of the material changes when it deforms under an external applied load. The shape of the structure can change if the deformation is large and the material properties will change for the same if the material reaches its failure limit. Whereas if the shift in the stiffness is very less during the entire deformation process, the assumption could be made that neither the shape nor the material property changes. This hypothesis forms the fundamental basic for linear analysis.

This hypothesis simplifies the problem design and its solution to a larger extend. Now, recalling the fundamental FEA equation,

$$[F] = [K] * [d] \quad (4)$$

Where: [F] is the known vector of nodal loads

[K] is the known stiffness matrix

[d] is the unknown vector of nodal displacements

The behaviour of the finite element models can be explained by the above matrix equation. Depending on the model size, the equation contains a high number of linear algebraic equations varying from thousand to several millions. The geometry, material properties and the restraints defines the stiffness matrix [K]. With the assumption for the linear analysis that the model stiffness stays the same, the equations are accumulated and resolved only one time, without the need of any updating throughout the model deformation. This method just takes an upright path from the problem origin to its completion. The results are obtained within a very short time even for large models.

For nonlinear analysis the entire scenario changes as the assumption of constant stiffness has to be abandoned. In this case throughout the deformation process of the material, stiffness changes and hence the stiffness matrix [K] needs to be updated as the nonlinear FEA solver advances over an iterative solution process. The amount of time to achieve the accurate result is considerably increased in this case considering the number of iterations

3.4 Types of Nonlinear behaviour

The possibility for the origin of the nonlinear behaviour in a structure cannot be explained easily even though the course of changing stiffness is same to all types of nonlinear analyses. Hence it is reasonable to classify the nonlinear analysis based on the principal origin of nonlinearity. Some analyses might have to account for more than a single type of nonlinearity since it is impossible to emphasise on only one cause of nonlinear tendency of structure in many problems.

3.5 Geometric nonlinearity

Like mentioned above, under operating conditions when the stiffness of the structure changes, the necessity of nonlinear analysis arises. If the change in shape of the structure forms the root cause for the stiffness variation, then the nonlinear behaviour is termed as geometric nonlinearity. The essence of such nonlinearity actually arises from relationship between strain and displacements (derivative of displacements).

Such deformation initiated stiffness variance occurs when the structure undergoes very large deformations that can be witnessed by naked eye. If the structure deformations are greater than $1/20^{th}$ of the largest dimension of the member, the call for nonlinear geometric analysis is made as per the generally accepted rule of thumb. In addition to that, for large deformations the load direction can also vary during the shape change. Two choices of loading: following and non-following are offered by most finite element analysis programs to account for this direction change of the loads.

The following load maintains its direction with respect to the deformed structure whereas the non-following loads maintains its initial direction

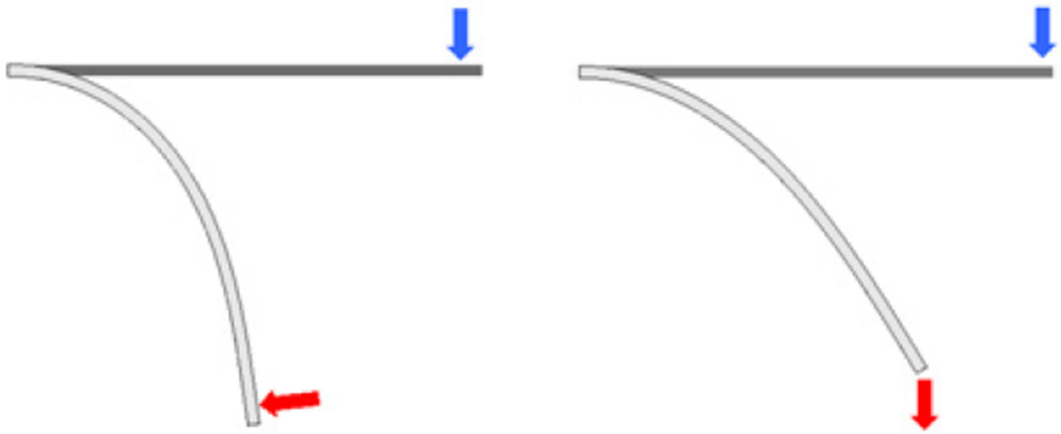

Figure 24 Following and non-following loads [6]

A pressure vessel that experiences a radical geometry change when subjected to very high pressure explains the concept of following and non-following loads. The pressure will act only normal to the walls of the structure. This scenario is analysed by the linear approach under the assumption that the shape of the structure remains same, whereas while considering the realistic approach the structure requires geometric nonlinear analysis with following (non-conservative) loads.

It is not necessary that the stiffness change occurs only for large deformations. There are cases where the stiffness change occurs for small deformations also. The below example demonstrates an initially flat membrane deflecting under pressure

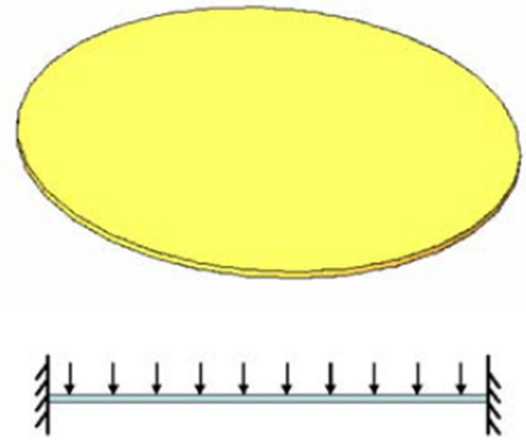

Figure 25 Thin membrane subjected to deflection under pressure [6]

This situation requires the necessity of nonlinear analysis even though the deformations are small. Primarily the membrane opposes the external pressure loads with bending stiffness only. Once the membrane starts deformation and reaches some curvature, an additional stiffness (due to nonlinear strain displacement equations) acts upon that get added along with the original bending stiffness. Hence the deformation modifies the membrane stiffness such that the deformed membrane is having even higher stiffness when compared to the flat membrane.

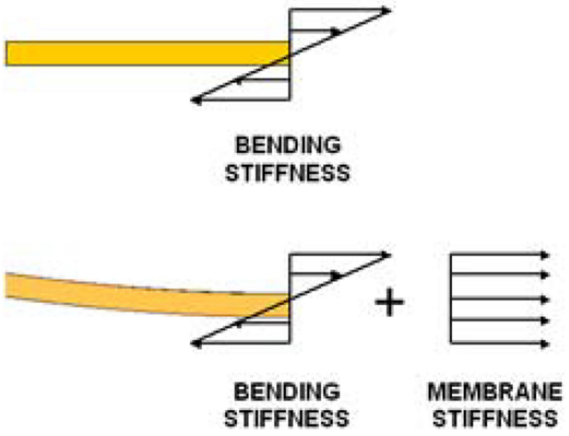

Figure 26 Stiffness change for small deformation [6]

3.6 Material nonlinearity

Material nonlinearity arises when the stiffness change is initiated only due to changes in material properties under loading conditions. For a linear model, the stress is assumed to be proportional to strain. In this case as the loading is increased the stresses and deformations also increases proportionally, and once the load is removed the model returns to its actual shape without any permanent deformation

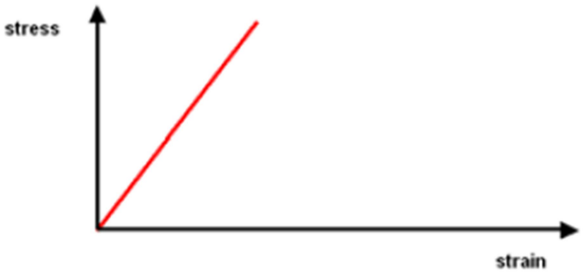

Figure 27 Linear stress-strain relation [6]

Even though the above mentioned simplification is tolerable, if the loadings are very high enough resulting in some permanent deformation of the structure as in the case with most plastic materials or for the case with rubbers and elastomers where strains are huge, then a nonlinear material model is to be used.

There are enormous differences in the material behaviour of various types of materials subjected to similar loadings. Hence the recent FEA programs have incorporated within them customised techniques and material models to simulate these behaviours. Below table shows such material model classification for FEM programs.

Table 5 Material models for FEA

Material classification	Model	Comments
Elastoplastic	Von Mises or Tresca	Strain-stress curve shows a 'plateau' before reaching the ultimate stress(Engineering metals & Some plastics)
	Drucker-Prager	Model for soils and granular materials
Hyperelastic	Mooney-Rivlin	Model for incompressible elastomers such as rubber.
	Blatz-Ko	Model for compressible polyurethane foam rubbers.
Viscoelastic	Several	Model for hard rubber or glass
Creep	Several	Time-dependent strain produced under a state of constant stress. Model for metals at elevated temperatures, high polymer plastics, concrete, and solid propellant in rocket motors
Super elastic	Nitinol	Model for shape-memory-alloys which shows super elasticity

3.7 Elastic stability loss (Buckling)

Stiffness of a material varies according to the external applied loads. At times depending on the application of loads material stiffness tends to increase(tension) or decrease(compression). For compressive loads if the variance in the stiffness is enough to cause the structure stiffness to fall off to zero, the state of buckling arises and rapid deformation of the structure is resulted. The stiffness then falls apart or attains a new stiffness in the post buckling state.

To calculate the Euler load or the Buckling load for the structure linear buckling analysis could be used. However, the results attained in this case wouldn't be conservative. Also, idealizations in the finite element model may result in the calculated buckling load for the structure to be much higher than the actual case scenario. Buckling may not always result in the catastrophic failure of the structure and the structure may be able to support the loads even

after the buckling mode. Only nonlinear analysis can explain the post-buckling behaviour of the structure.

3.8 Contact stresses and nonlinear supports

Nonlinear analysis is to be performed if the support conditions including contacts vary during the application of external operating loads. Between two contacting surfaces, contact stresses are developed. Hence the area of contact and the corresponding stiffness are not known prior to solution. The need for nonlinear analysis arises as the stiffness of the contact zone varies even though the contact stress area is very small compared to the original model shape.

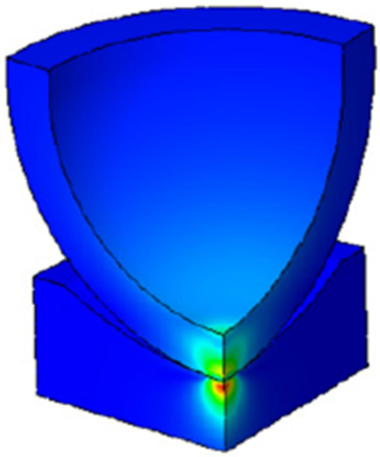

Figure 28 Contact stresses formation [6]

Nonlinear supports also calls for the performance of nonlinear supports at times. The figure below demonstrates such a situation where effective beam length and its corresponding stiffness depend on the amount of beam deformation. The stiffness is increased when the beam element contacts the support due to reduction in active length

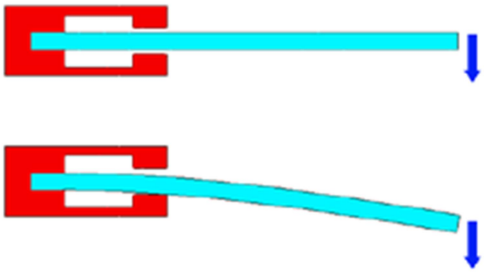

Figure 29 Effect of support in nonlinearity [6]

3.9 Dynamic analysis-Nonlinear

Inertial effects, time-dependant loads and damping are usually accounted by dynamic analysis. Hence engineering problems like crash stimulation or airbag deployment, drop test, vibrations of an engine mount etc. require dynamic analysis.

Under the applied load, if the model stiffness does not vary significantly then linear dynamic analysis is enough. In case of a tuning fork or a vibrating mount, small vibrations about the point of equilibrium are experienced and hence performance of linear dynamic analysis is enough whereas for problems like analysis of airbag deployment, crash simulations or modelling a metal stamping process etc. needs nonlinear dynamic analysis to be performed since large deformations and finite strains (nonlinear geometry) and material nonlinearity should be accounted for.

4. SOFTWARE TOOLS

4.1 MSC Patran

One of the recent, widely used pre/post processing software in the field of finite element analysis (FEA) is MSC Patran. This tool can provide solid modelling, meshing, analysis set up etc. to solvers including Abacus, MARC, Nastran, LS-DYNA, ANSYS etc.

In this research Patran is used to model and mesh the sea gate section considered which will be exported to MSC MARC for the further analysis.

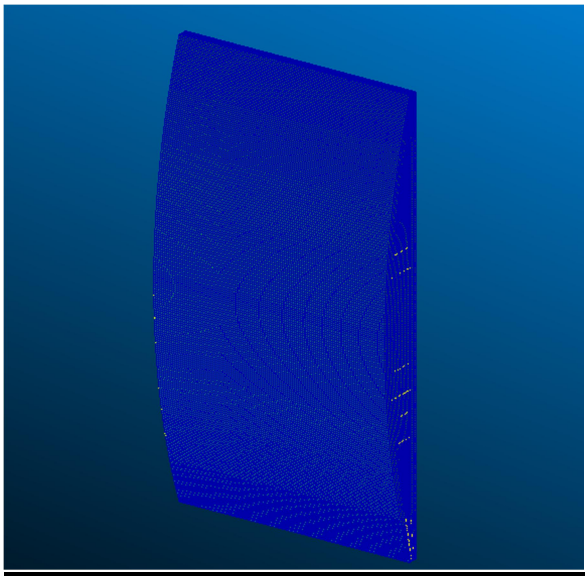

Figure 30 Sea Gate section modelled and meshed in Patran

Figure 30 shows the sea gate section that was modelled, meshed and ready to be extracted to MSC MARC.

4.2 MSC MARC

MSC MARC is general purpose nonlinear finite element analysis software against static, dynamic and multi-physics loading cases. The software is widely used these days and is very powerful. Different complex design problems can be easily dealt with MARC due to its ability to easily model nonlinear material behaviour.

The software can easily simulate all types of nonlinearities including material, boundary condition, geometric etc. It provides a robust nonlinear solution and also helps to predict failure, damage and crack propagation. The software also helps to bridge between electrical, thermal, magnetic and structural analyses. All nonlinear requirements for simulation are easily carried out by this software.

The software with its wide range of applications helps in variety of engineering solutions including,

- All types of nonlinear analysis
- Electromagnetics
- Piezoelectric analysis
- Thermal analysis
- Coupled thermo mechanical analysis
- Electrostatics and Magneto statics coupled with structural response
- Electrical-Thermal-Mechanical
- Piezoelectric analysis with higher order 3D elements
- Manufacturing processes like sheet metal forming, hydroforming, extrusion, blow moulding, welding, induction heating, quenching, curing, cutting etc.

In this research, the meshed model of the Sea Gate section from MSC Patran is exported to MSC MARC for the performance of nonlinear analysis. The loading cases provided by the designer company along with the manually calculated belt force will be applied on to the structure in the software and the structural behaviour is analysed. It is then followed by the Ultimate strength determination of the structure using nonlinear FEM. The results extracted from the analysis are included in this report

5. STRUCTURAL ANALYSIS

5.1 Modelling and Meshing

From the provided drawings including the profile views and the sectional views by the designer company Marsima, finite element modelling of the sea gate structure were carried out. The FEA tool used for this is PATRAN from MSC. The structure was modelled as surfaces including for the plates and stiffeners from base, no beam elements were used. The surfaces were generated by creating the curves and then extruding them. The material properties for the steel structure including the elastic modulus, Poisson's ratio and density were assigned using the isotropic properties.

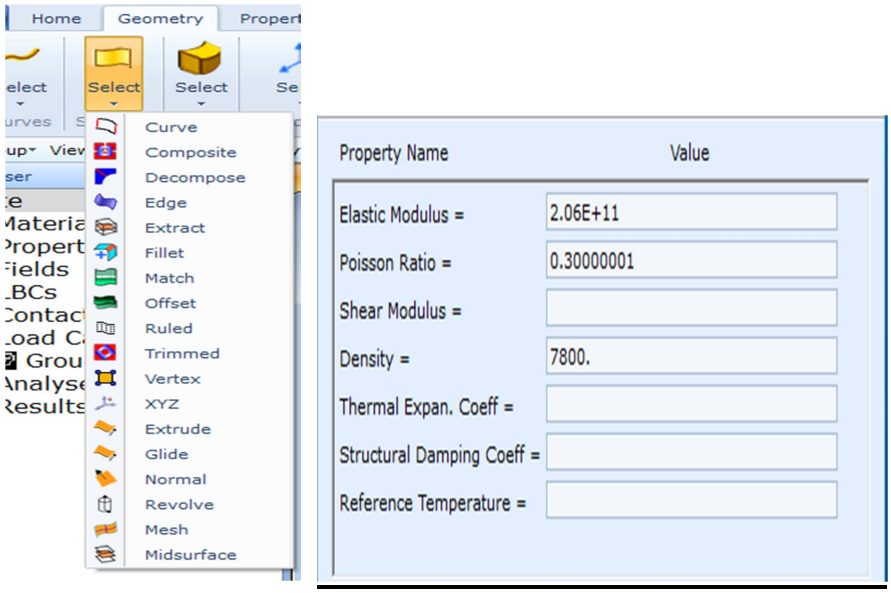

Figure 31 Surface generation and material property description

This time the belt associated with the structure was not modelled along with the structure itself, instead the effect of the model on the structure is calculated manually and applied on the structure as force externally.

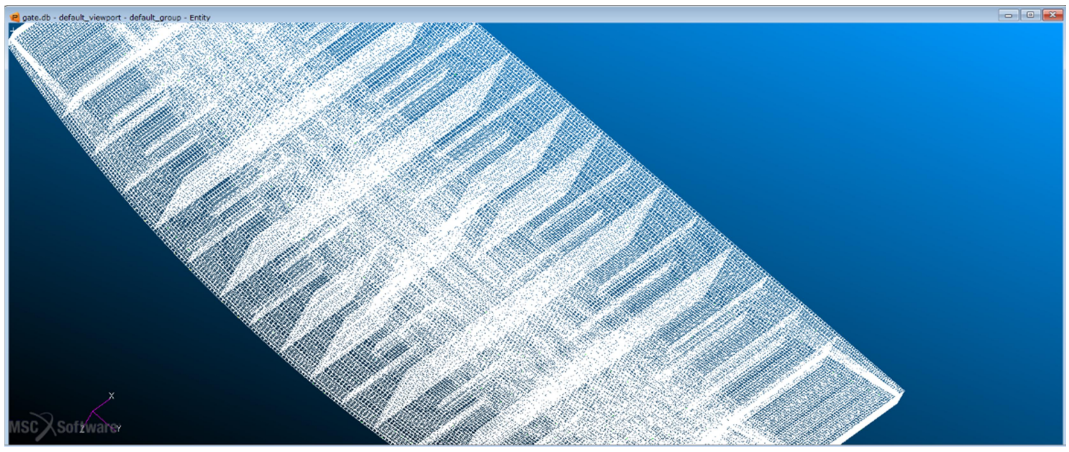

Figure 32 Meshed structure

The mesh was generated using the quadrilateral elements. The main points kept in consideration for the meshing are

- To follow an aspect ratio of 1 for the elements wherever possible; however for complex areas however this could not be achieved
- To maintain the proper sharing of nodes between the side walls and the intersecting elements to attain proper mesh integrity

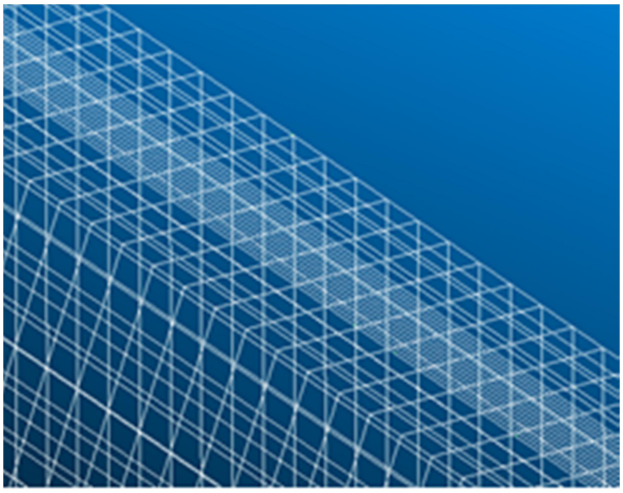

Figure 33 Mesh quality, closer view

Finally, the full finite element model is developed as shown in Figure 34

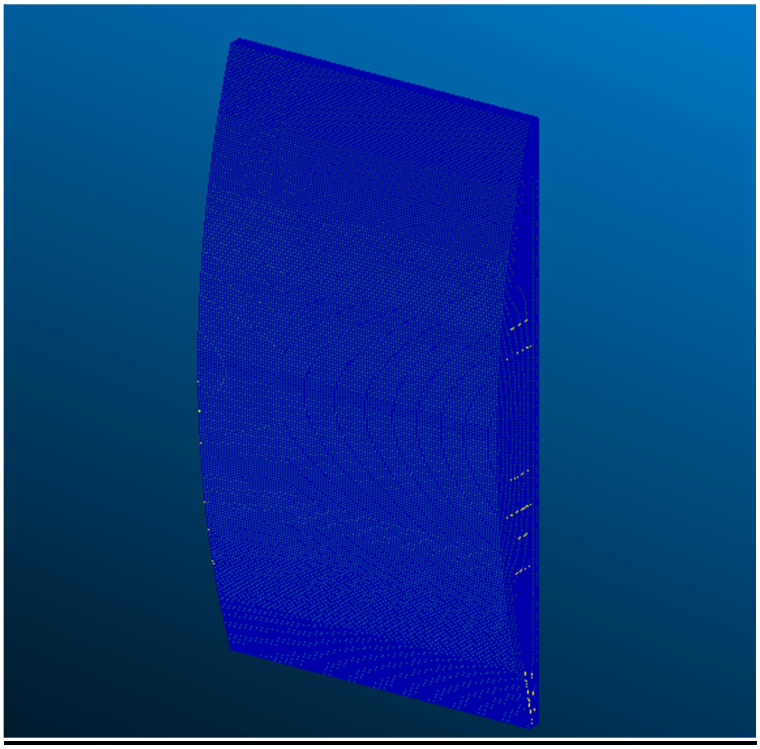

Figure 34 Final FEM model

5.2 Eigen value analysis

[7] Determining the natural frequencies and different mode shapes of the structure (considering no damping) is the usual first step carried out while performing dynamic analysis. The basic dynamic behaviour of the structure and the structural response for the same when encountered with dynamic loads could be characterised by this.

If a structure is subjected to disturbance, the frequency at which the structure tends to naturally vibrate is termed as its natural frequency. Fundamental frequency, resonant frequency, characteristic frequency, normal frequency etc. are the other terminologies used for the natural frequency. The deformed shape of the structure, at any particular natural frequency is termed as its normal mode of vibration for the corresponding frequency. Hence each mode shape is associated with a specific natural frequency.

Mode shapes and natural frequencies are functions of boundary conditions and structural properties. For instance, in the case of a cantilever which has its natural frequencies and associated modes of vibration; when subjected to structural property change, will lead to the change in the natural frequency change only and not necessarily mode shape change. For example if the elastic modulus of the cantilever beam is changed, it will lead to the change in natural frequency whereas the mode shapes remain the same. But for the same cantilever is subjected to boundary condition change, it leads to both natural frequency and mode shape change.

5.2.1 Reasons to compute normal modes

Natural frequencies and normal modes computation are important for many reasons. The dynamic interaction between the structure and its support can be evaluated using this. For instance, to install a rotating fan on the ceiling of a building the operating frequency of the fan is to be evaluated and made sure that it is nowhere close to one of the natural frequencies of the building. If the frequencies match during the operation of the fan, there is a high chance that the structure might lead to structural damage or failure.

The natural frequency analysis helps to judge the decisions regarding subsequent dynamic analysis (i.e. frequency response, response spectrum analysis, transient response etc.). To choose the most suitable frequency step or time for integrating the equations of motions, the major modes can be evaluated. Likewise, the results of Eigen value analysis-the mode shapes and natural frequencies can be used in modal frequency and modal transient response analysis.

The dynamic analysis results are sometimes compared with the physical test results. To guide the experiment a normal mode analysis can be used. Before the experiment a normal mode analysis could be used to fix the location of accelerometers and after the experiment it could be used as a mean to correlate the results between the analysis and the test results. Once the natural frequency and the normal modes are known, design changes are also even possible for the structure.

There are several uses of calculating the natural frequencies and the mode shapes for a structure. And hence the real Eigen value analysis forms the basis for many types of dynamic response analysis. It can be summarised that for all types of dynamic analysis, an overall understanding of the normal modes analysis as well as knowledge of natural frequencies and mode shapes are needed.

5.2.2 Overview of normal modes analysis

A special reduced form of equation of motion is needed for the solution of equation of motion for the natural frequencies and normal modes or Eigen modes. If the applied loading and damping are neglected, the equation of motion in matrix form reduces to

$$[M]\{\ddot{u}\} + [K]\{u\} = 0 \qquad (5)$$

Where [M] = mass matrix

[K] = stiffness matrix

The above equation represents equation of motion for undamped free vibration. For solving this, harmonic solution is assumed which is of the form

$$[u]=\{\varphi\}\mathrm{Sin}\,\omega t \qquad (6)$$

Where $\{\varphi\}$ = Eigen vector or Mode shape (amplitudes of motion)

ω = Circular natural frequency

The harmonic form becomes the main key factor for the numerical solution of the equation. Apart from that it also has a main physical significance which is all the degrees of freedom of the vibrating structure follows as synchronous moving tendency. During motion, the structural configuration does not change its basic shape; it is also the amplitude which changes.

Differentiating the assumed harmonic solution and substituting it into the equation of motion, we get

$$-\omega^2[M]\{\varphi\}\sin\omega t+[K]\{\varphi\}\sin\omega t=0 \quad (7)$$

On further simplification we get,

$$([K]-\omega^2[M])\{\varphi\}=0 \quad (8)$$

This is a set of homogenous algebraic equations for the components of Eigen vector and is termed as Eigen equation. This forms the basis for the Eigen value problems. An Eigen value problem is considered as a specific equation that has wide range of applications in linear matrix algebra. Eigen value problem in its basic form can be represented as

$$[A-\lambda I]X=0 \quad (9)$$

Where A = Square matrix

λ = Eigen values

I = Identity matrix

X = Eigen vector

In structural analysis, the physical representations of the natural frequencies and mode shapes are resulted from the representations of stiffness and mass in the Eigen equation. Hence the Eigen equation is written in the form which includes K, w and M with $w^2 = \lambda$ as shown in equation (4)

For equation (4) the only possible outcomes are

1. If det $([K]-\omega^2[M]) \neq 0$, then the only possible solution is

$$\{\varphi\}=0 \quad (10)$$

This trivial solution represents the case of no motion and doesn't help really to understand any physical interpretation.

2. If det $([K]-\omega^2[M]) = 0$,

In this case a non trivial solution is obtained for

$$([K] - \omega^2[M])\ \{\varphi\}=0 \qquad (11)$$

The general mathematical Eigen value problem reduces to one of solving the equation of the form from a structural engineering point of view.

$$\det([K]- \omega^2[M]) = 0 \qquad (12)$$

or

$$\det([K]- \lambda\,[M]) = 0 \qquad (13)$$

where $\lambda = \omega^2$

The determinant is zero only at a set of discrete Eigen values λ_i or ω^2_i. The Eigen vector $\{\varphi_i\}$ satisfies equation (7) and corresponds to each Eigen value. Hence equation (7) can be rewritten as

$$([K] - \omega_i^2[M])\ \{\varphi_i\}=0 \quad i=1,2,3.. \qquad (14)$$

Free vibration mode of the structure is represented by each Eigen value and Eigen vector. The i^{th} natural frequency can be related to the i^{th} Eigen value as

$$f_i = \omega_i/2\pi \qquad (15)$$

where $f_i = i^{th}$ natural frequency

$\omega_i=(\lambda_i)^{1/2}$

The number of Eigen vectors and Eigen values is equal to the number of dynamic degrees of freedom or the number of degrees of freedom that have mass.

In various dynamic analyses, different characteristics of mode shapes and natural frequencies become useful. First, the deflected shape of a linear elastic structure vibrating in free or forced vibration has a deflected shape at any given time which is a linear combination of all its modes.

$$[u] = {}_i\Sigma\{\varphi_i\}\xi_i \quad (16)$$

Where $[u]$ = vector of physical displacements

$\{\varphi_i\}$ = i^{th} mode shape

ξ_i = i^{th} modal displacement

Second, if [M] and [K] are real and symmetric, which is the case for all common structural finite elements, the below mathematical properties hold.

$$\{\varphi_i\}^T [M] \{\varphi_j\} = 0 \quad \text{if } i \neq 0 \quad (17)$$

$\{\varphi_i\}^T$ [M] $\{\varphi_j\}$ = mj = jth generalised mass

5.2.3 Eigen value analysis for sea gate section

The meshed model of the sea gate structure is imported into MSC MARC to perform the Eigen value analysis. This is done to evaluate the first few mode shapes and the corresponding natural frequencies of the structure.

Boundary conditions are given as shown below for the four sides of the section and the corresponding nodes involved.

Table 6 Boundary conditions

Boundary Conditions	Translations in directions			Rotations around axes		
	x	y	z	x	y	z
Top	fixed	fixed	fixed	open	open	open
Bottom	fixed	fixed	fixed	open	open	open
Side 1_Symmetric	fixed	open	open	open	fixed	fixed
Side 2_Symmetric	MPC	open	open	open	fixed	fixed

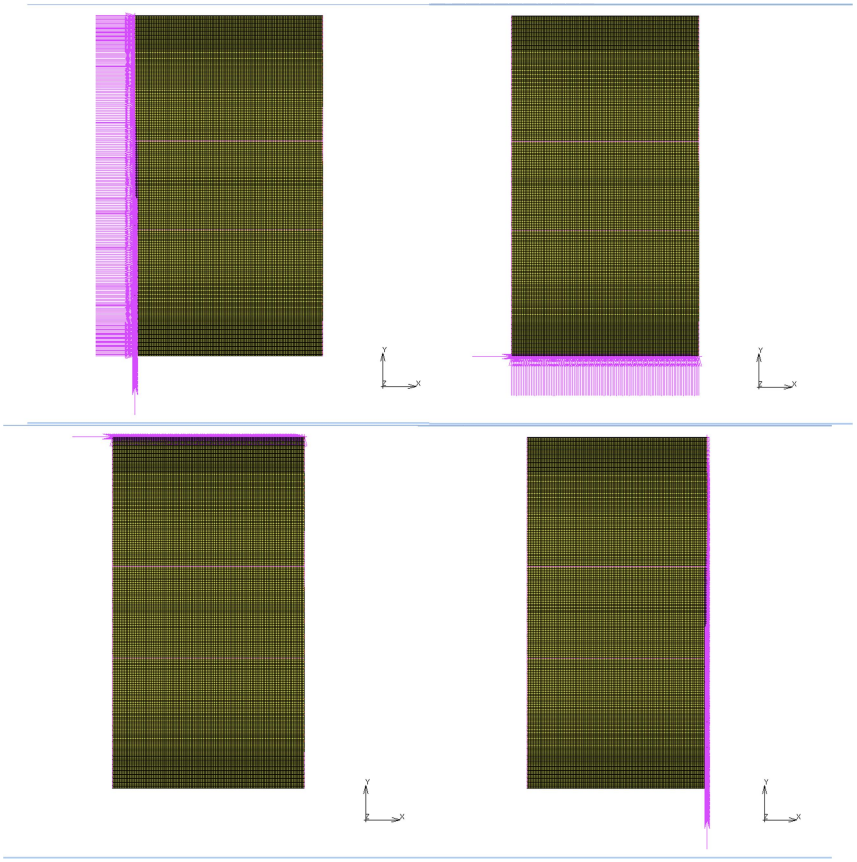

Figure 35 Boundary conditions applied on the structure

Eigen value analysis is performed and the first few modes and the corresponding natural frequencies are found out for the considered sea gate section. The following figures show the first three mode shapes and their corresponding frequencies for the section.

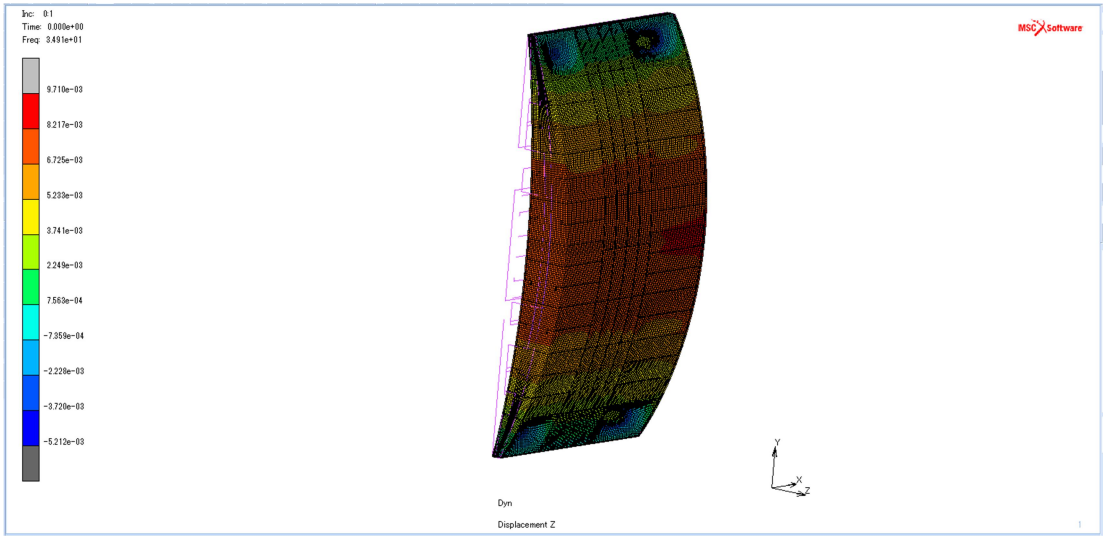

Figure 36 First mode shape

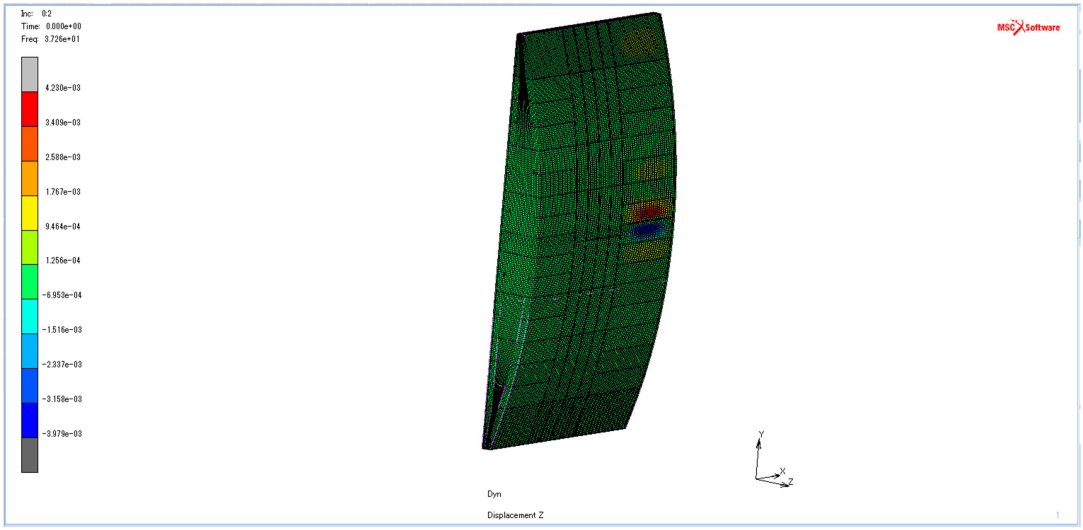

Figure 37 Second mode shape

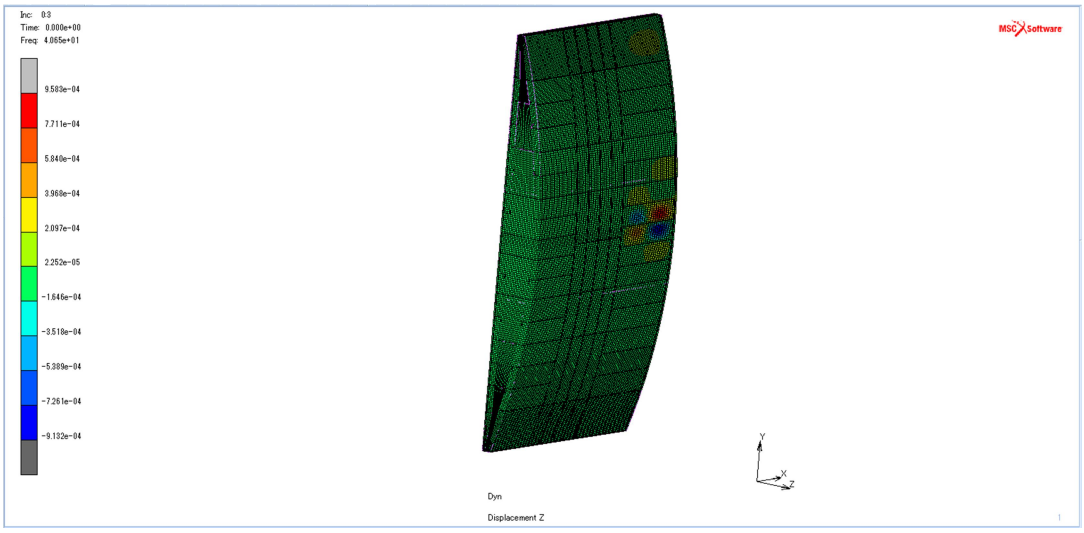

Figure 38 Third mode shape

The idea behind the performance of Eigen value analysis is to determine the first natural frequencies of the structure and to compare it with the Tsunami wave impact period recorded during the model test for the structure. The converted large scale results will be calculated and compared.

The first three mode shapes obtained from the analysis and the corresponding natural frequencies/time periods are tabulated below.

Table 7 Mode Shapes, frequencies & time period

Mode Shape	Corresponding NF(Hz)	Time Period(s)
1	34.91	0.029
2	37.28	0.027
3	40.65	0.025

5.2.4 Data extraction and comparison with model test results

The functionality test of the model with scale factor of 1/200 is already being performed in the Kyoto University, Japan. The following figure shows the results with the belt tension in the model plotted against the time elapse of the model Tsunami wave generated in the Tsunami flume.

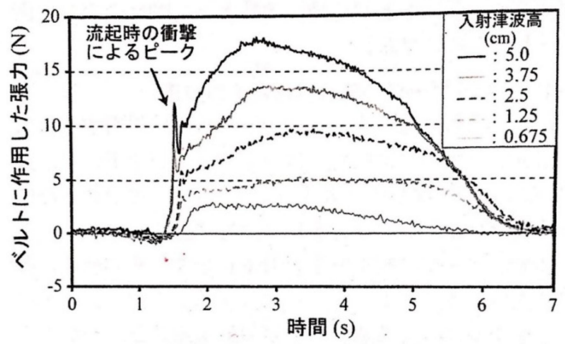

図-9 ベルトに作用する張力（波力）の時系列データ（4つのひずみゲージの測定値を合算）

Figure 39 Model test result(1/200)

At around 1.5 seconds of time we see a sudden rise in the belt tension. This is happening because of the impact load from the Tsunami wave, which causes the sea gate to stand erect. It is then followed by the long period Tsunami wave. From the figure it is clear that the time period for the impact model Tsunami load is around 0.25seconds. Converting this time period into real scale model, we get t=3.53 seconds.

Now when we compare the time periods corresponding to the natural frequencies of the first three modes of vibration of the structure to the impact load time period of the Tsunami wave, it is in no range.

Table 8 Time period comparison

	Structure Modes			**Tsunami Impact load**
	1	**2**	**3**	
Time period(s)	0.029	0.027	0.025	3.53

From Table 7 it is clear that the time period/natural frequency for the first three modes of structure vibration is in no range of the impact load period for the Tsunami wave. Hence the non-necessity of the dynamic analysis is proved.

5.3 Loading

The design of the structure is done by Marsima Aqua system, Japan. Now to check the structural behaviour of the design, the company has provided with different loading conditions. These loading conditions include both Level 1(L1) Tsunamis and Level 2(L2) Tsunamis, three cases; case 1, case 2 & case 3 for both L1 & L2 type Tsunamis.
The following table shows the different cases of loading to be analysed.

Table 9 Loading cases

Tsunami Type	Case	Return period(years)
Level I(L1)	1	100
	2	100
	3	100
Level II(L2)	1	1000
	2	1000
	3	1000

The loads cases, both L1 & L2 are calculated based on the Tanimoto expressions.

5.3.1 Tanimoto Expressions

[8] In 1984, Tanimoto et al. suggested a pressure formula for the non soliton fission Tsunami waves acting on a vertical wall. The following equations represent the same.

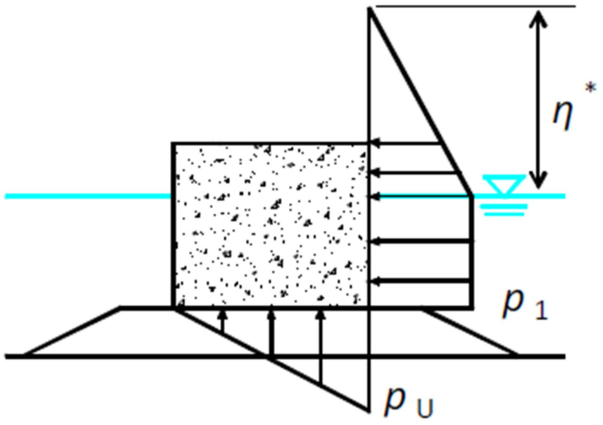

Figure 40 Pressure distributions in existing formulas [8]

$$\eta^* = 3.0a_I \quad (18)$$

$$p_1 = 2.2\rho g a_I \quad (19)$$

$$p_u = p1 \quad (20)$$

Here η^* is the wave pressure acting height, p_1 is the wave pressure acting horizontally under the still water level, p_u is the caisson toe uplift pressure respectively. Incident Tsunami wave height is represented by a_I and ρ is the density of water. However for soliton fission Tsunami, modified Tanimoto formula was proposed by the Guidelines for tsunami-resistant design of Breakwater (MLIT, 2013). In this update, the coefficient of 2.2 for p_1 is substituted by 3.0 as represented in the following equation.

$$p_1 = 3.0\rho g a_I \quad (21)$$

This increase in the horizontal pressure corresponds to the impulsive pressure due to soliton fission.

5.3.2 Load Cases

Different Load cases are already being provided by the designer company Marsima. These loading cases will be used to evaluate the structural behaviour of the sea gate section using nonlinear FEM.

- Level I – Case 1 (L1C1)

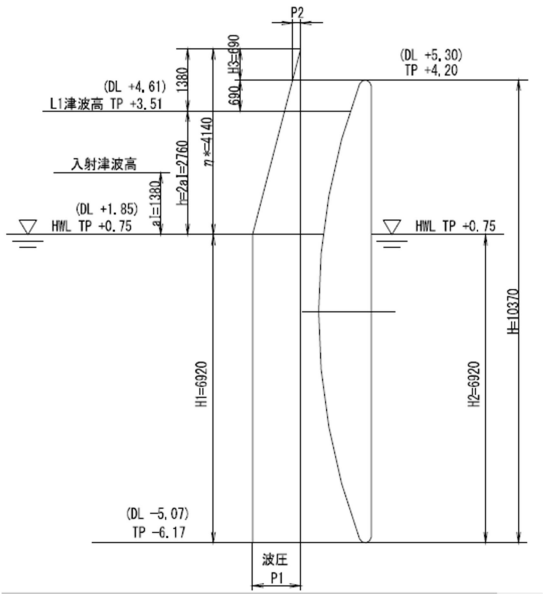

Figure 41 L1C1 loading

P1 = 30.664 kN/m^2, P2 = 5.111 kN/m^2

- Level I – Case 2 (L1C2)

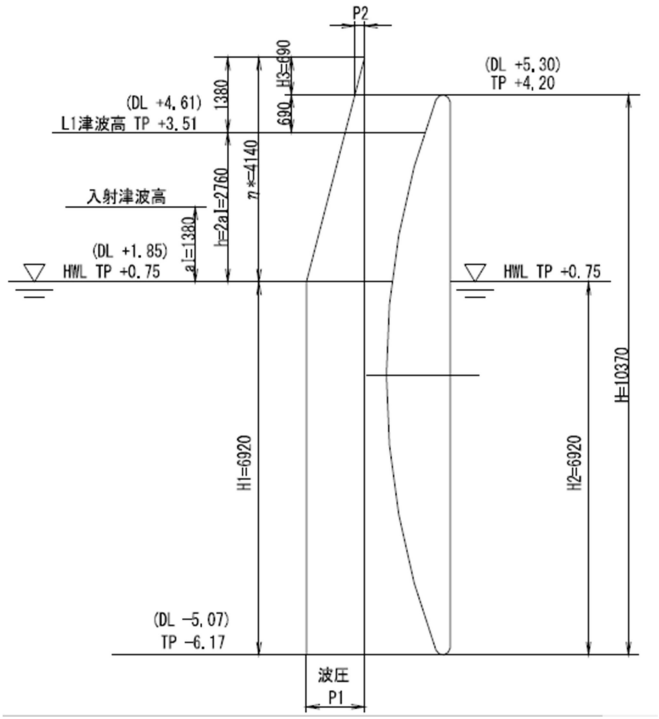

Figure 42 L1C2 Loading

$P1 = 61.327\ kN/m^2$, $P2 = 35.774\ kN/m^2$

- Level I – Case 3 (L1C3)

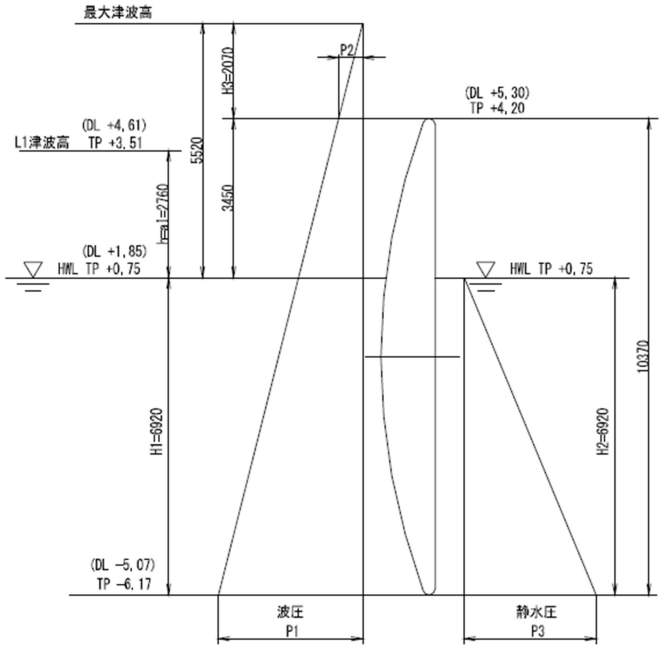

Figure 43 L1C3 Loading

$P1 = 131.926\ kN/m^2$, $P2 = 21.952\ kN/m^2$, $P3 = 62.903\ kN/m^2$

- Level II – Case 1 (L2C1)

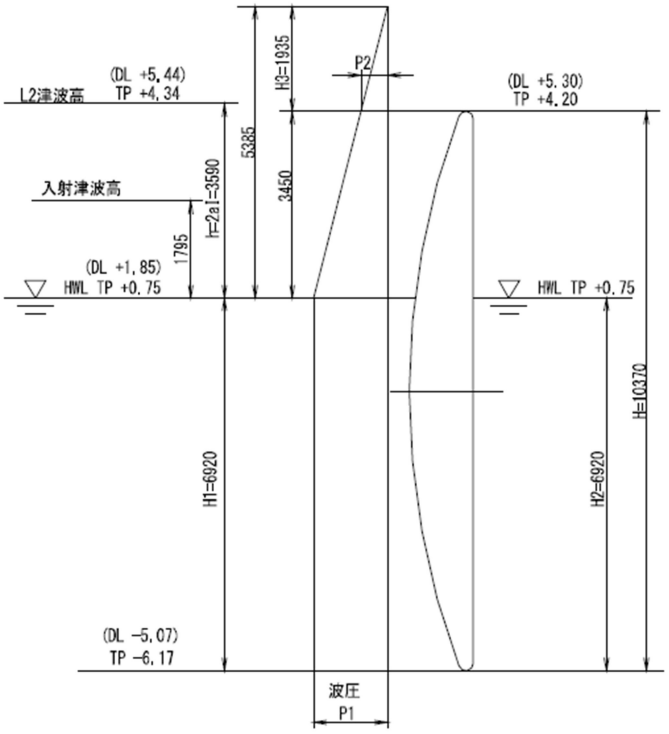

Figure 44 L2C1 Loading

P1 = 39.885 kN/m^2, P2 = 14.332 kN/m^2

- Level II – Case 2 (L2C2)

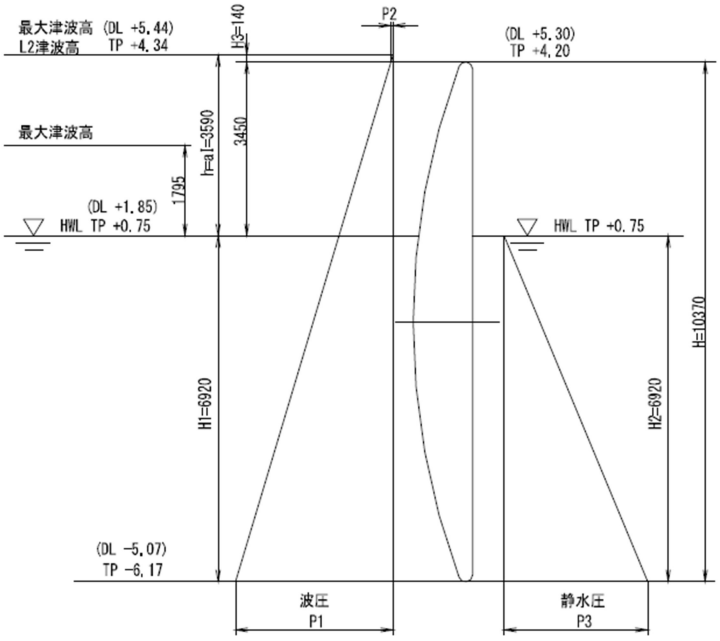

Figure 45 L2C2 Loading

P1 = 111.459 kN/m^2, P2 = 1.485 kN/m^2, P3 = 62.903 kN/m^2

The Level II – case 2(L2C2) loading case is used as the design loads for the sea gate structure by the designer company.

- Level II – Case 3 (L2C3)

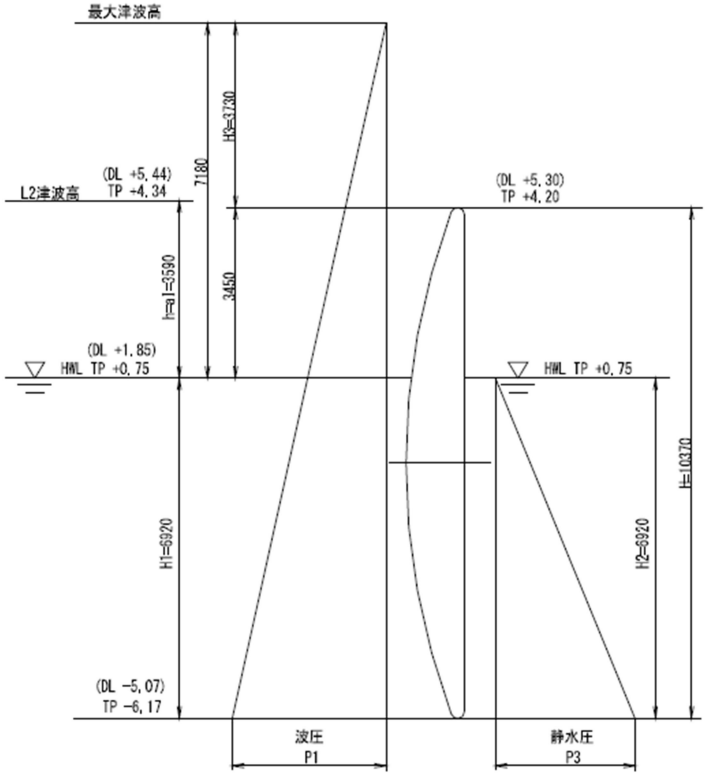

Figure 46 L2C3 Loading

P1 = 149.531 kN/m^2, P2 = 39.557 kN/m^2, P3 = 62.903 kN/m^2

5.3.3 Evaluation of belt loads

There is a belt attached to the Sea gate structure, which keeps the structure vertically standing on the application of the Tsunami loads. However in my research the belt will not be modelled along with the structure and analysed, instead the effect of belt will be manually calculated and applied as load/pressure on to the structure. This is done to avoid the complexity of the analysis and to get the proper results.

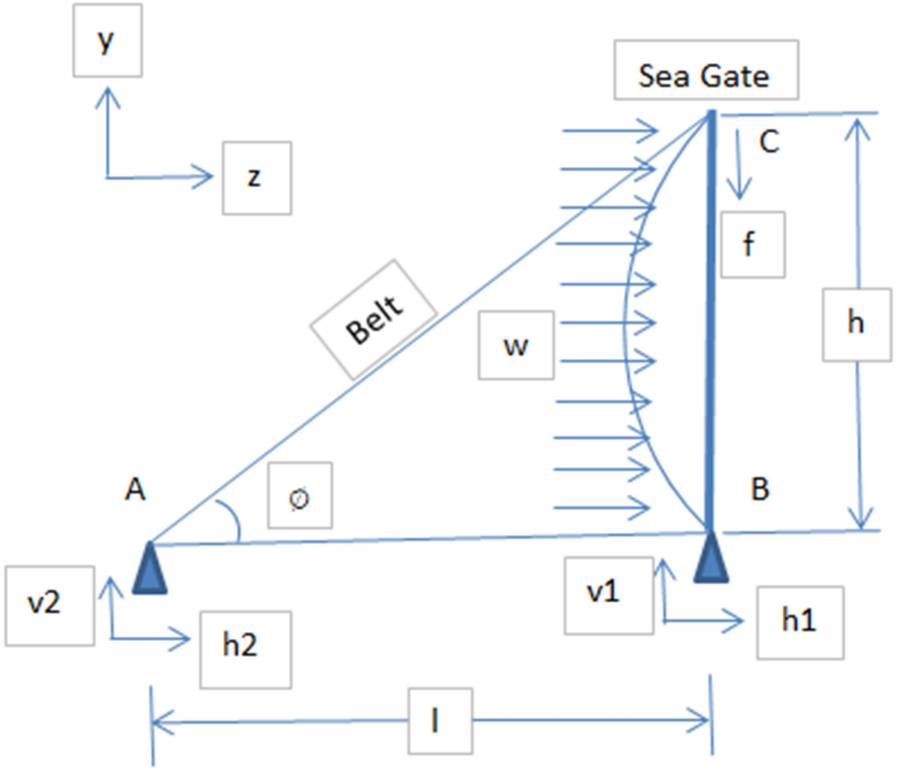

Figure 47 Belt Pressure calculation

Here v1, v2 h1 & h2 are the reaction forces developed at A and B; h is the height of the structure and l is the reach of the belt; w is the assumed uniform pressure acting on the structure and f is the internal force developed at C that is vertically acting on the structure.

Assuming the belt associated with the Sea gate structure to be rigid and a uniform pressure of w is acting on the structure as shown in figure 40, the equilibrium of forces can be written as

$$h1 + h2 + wh = 0 \quad (22)$$

$$v1 + v2 = 0 \quad (23)$$

Taking moment around point B,

$$(wh^2)/2 + v2l = 0$$

Also,

$$\tan(\emptyset) = (h/l) = (v2/h2) \quad (24)$$

Solving the above equations,

$$h1 = (wh)/2 \quad (25)$$

$$h2 = (l/h)v2 = -(wh)/2 \quad (26)$$

$$v1 = (wh^2)/(2l) \quad (27)$$

$$v2 = -(wh^2)/(2l) \quad (28)$$

Due to the reaction forces an internal force f from the belt will be acting vertically down on to the structure.

$$f = -(v1) \quad (29)$$

The same principle is applied to manually calculate the effect of belt on to the structure for every loading case available. The force thus calculated is applied as pressure on the topside of the structure where the belt is acting. Below table shows the values of pressure that was manually calculated for each case based on the above.

Table 10 Pressure due to belt force

Tsunami Type	Case	Pressure (kN/m2)
Level I	1	1099.30
	2	2557.35
	3	2342.11
Level II	1	1537.77
	2	1368.89
	3	3179.24

5.4 Boundary conditions

The following boundary conditions are applied, for the non-linear static analysis.

Table 11 Boundary conditions

Boundary Conditions	Translations in directions			Rotations around axes		
	x	y	z	x	y	z
Top	open	open	fixed	open	open	open
Bottom	open	fixed	fixed	open	open	open
Side 1_Symmetric	fixed	open	open	open	fixed	fixed
Side 2_Symmetric	MPC	open	open	open	fixed	fixed

5.5 Non-linear Analysis

Once the model is ready and the boundary conditions are applied, the elasto-plastic material properties are inputted. The properties are described as shown below and inputted in the software. Since the Tsunami loads are intense/extreme loads the structure will be subjected to geometric non-linearity and hence nonlinear analysis is performed.

Table 12 Material Properties

Material Properties	
Young's modulus(N/m2)	2.06*10^(11)
Yield strength(N/m2)	2.4*10^(8)
Poisson's ratio	0.3

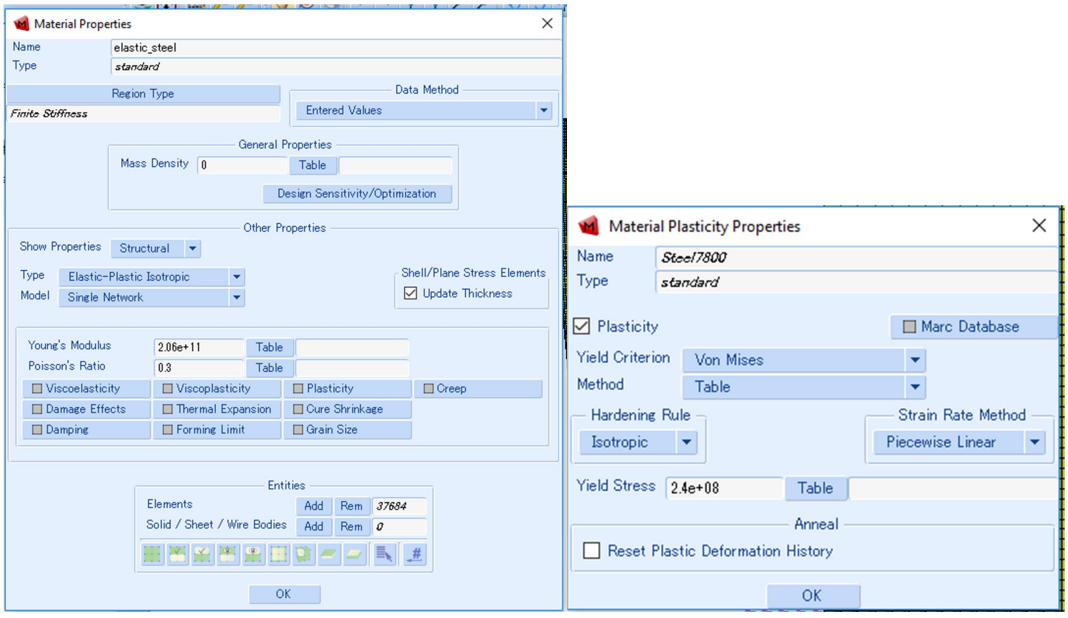

Figure 48 Material Properties in MSC MARC

Once the material properties are given, loading is given. The loading/pressure values provided by the designer company is applied on the structure as face loads. Three cases each for L1 and L2 type of Tsunamis are applied to analyse the behaviour of the structure. The effect of the belt, calculated in section 5.3.3 is also applied vertically on top of the structure.

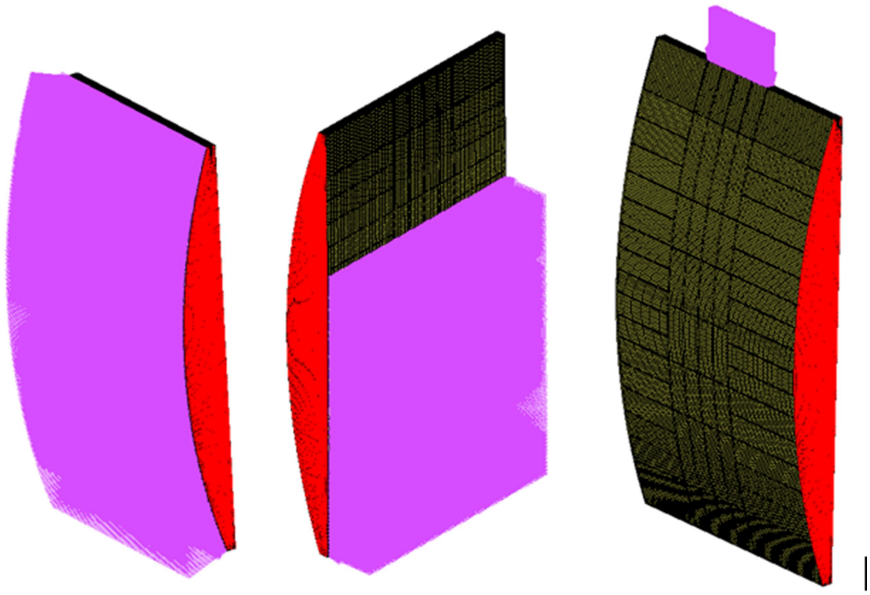

Figure 49 Pressure applied as face load on the structure

For the application of the loads, arc length method is used which allows the gradual increment of loadings from zero loading.

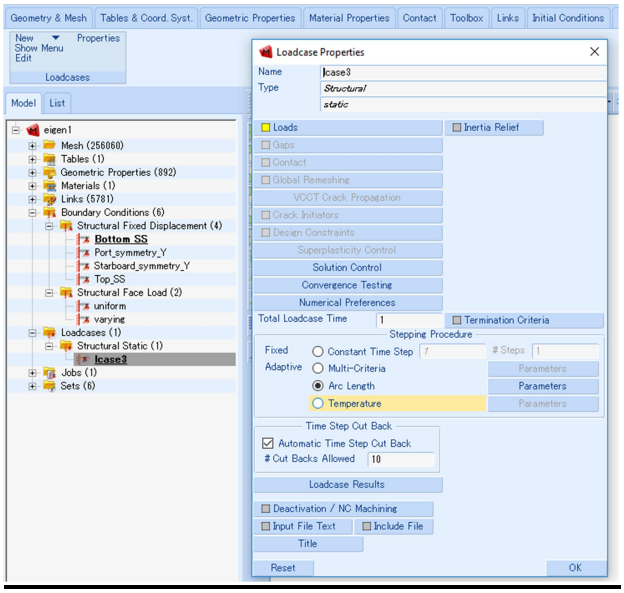

Figure 50 Solution parameters

The static analysis are performed for each loading conditions, L1 and L2. To check the successful completion of every analysis the following run job summary is evaluated. Once it shows the status to be complete with an analysis time of 1 and an exit number of 3004, it can be finalised that the analysis converged and is successful.

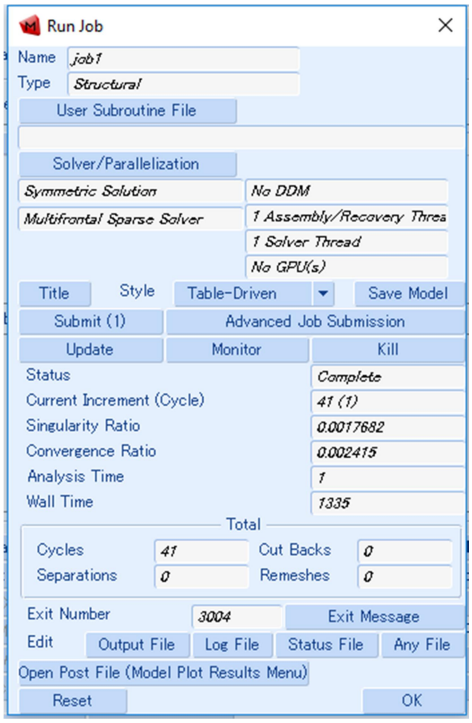

Figure 51 Analysis review

5.6 Results overview

Since the structure is having yield strength of 240 MPa and the design philosophy for the structure is different in case of both level 1 and level 2 types of Tsunamis, the Von Mises stress and the equivalent plastic strain in the structure will be mainly evaluated for each case.

For both Level I and Level II loading cases, the design philosophy for the structure are different, hence the result checking criteria will also vary.

For the Level I loading only elastic deformation of the whole structure is allowable, the structure should lie in the elastic region in the stress-strain graph whereas for Level II loading case, the structure can actually undergo plastic deformation while keeping its functionality.

For Level I loading cases, the structure should be totally maintained whereas for Level II loading partial structure of the breakwater only needs maintained.

5.6.1 Level I – Case 1

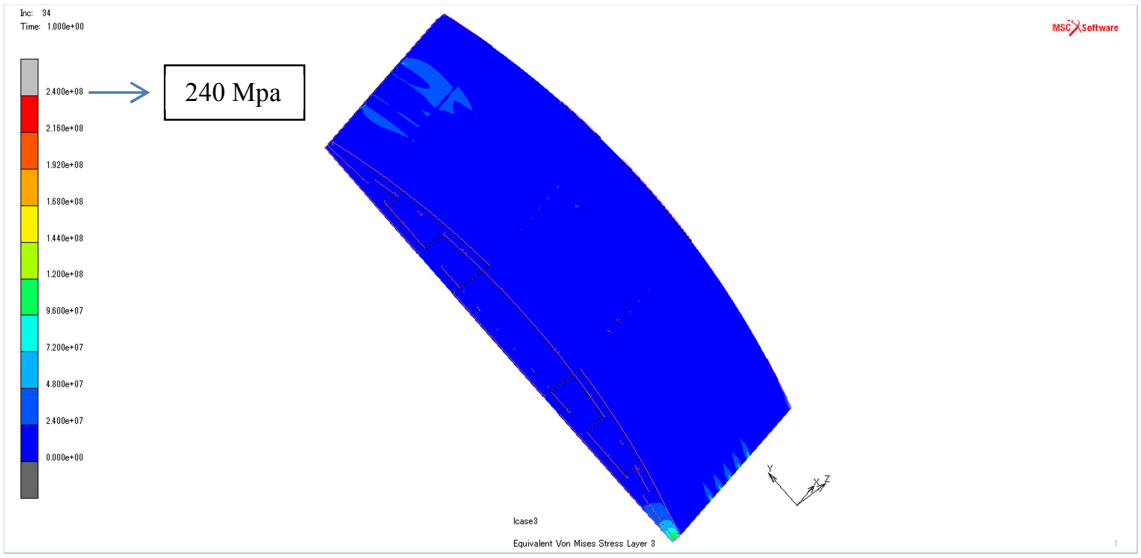

Figure 52 Von Mises stress distribution_Level 1_Case1

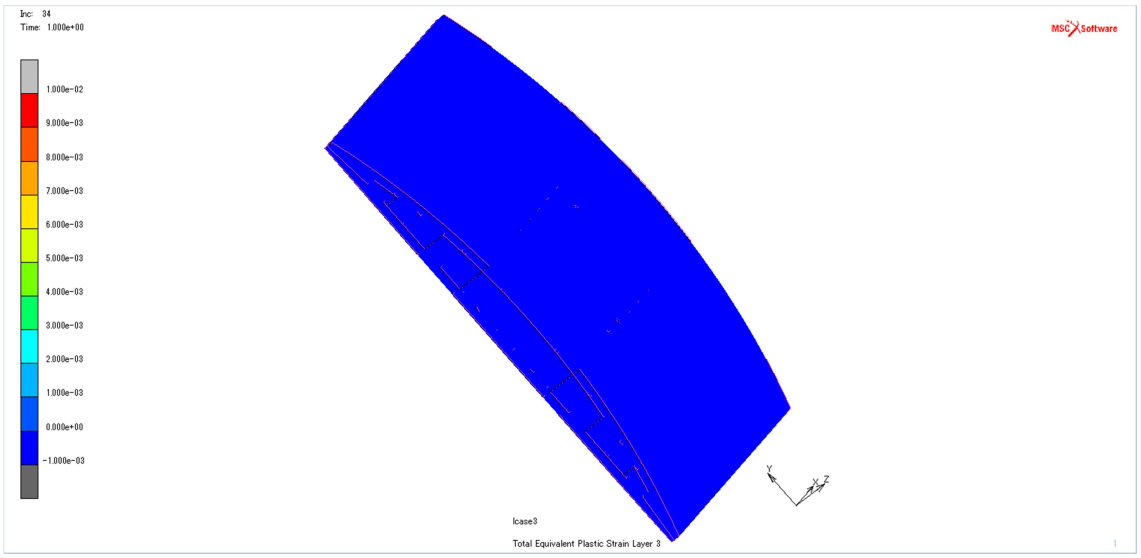

Figure 53 Equivalent Plastic strain_Level 1_Case1

Figure 52 shows the Von Mises stress distribution happening in the structure when subjected to Level 1 – case 1 loading. The Von Mises stresses are very low in the structure; the maximum range of stresses visible is in between 24 MPa ~ 48 MPa. This stress however is developed due to the boundary effect and hence it could be neglected.

Figure 53 shows the equivalent plastic strain happening in the structure. It is very clear that the structure stays within the elastic range without any plastic deformation. To conclude, the structure is safe against L1C1 loads and it follows the design philosophy.

5.6.2 Level I – Case 2

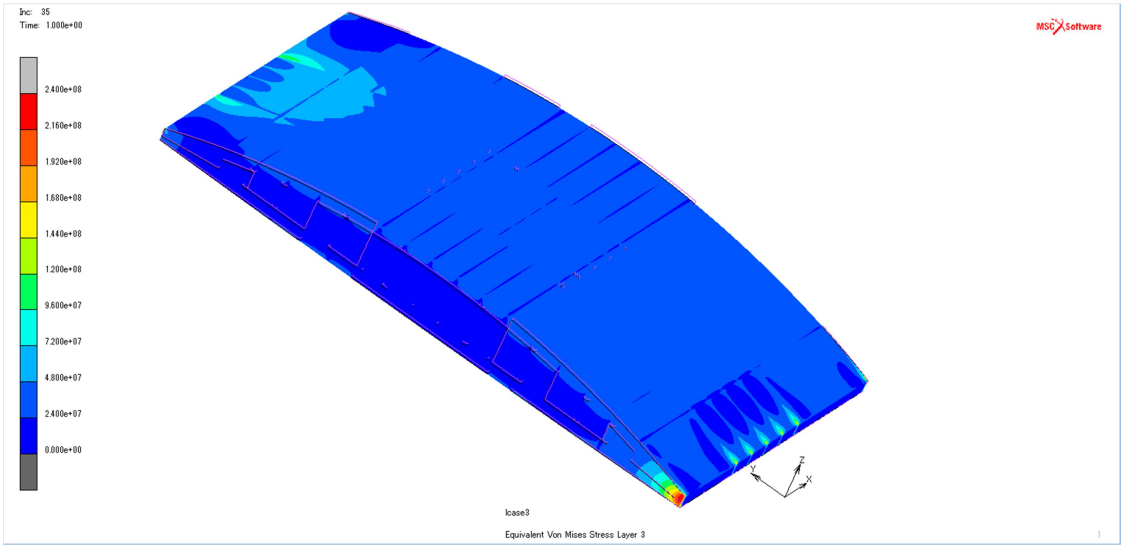

Figure 54 Von Mises stress distribution_Level 1_Case 2

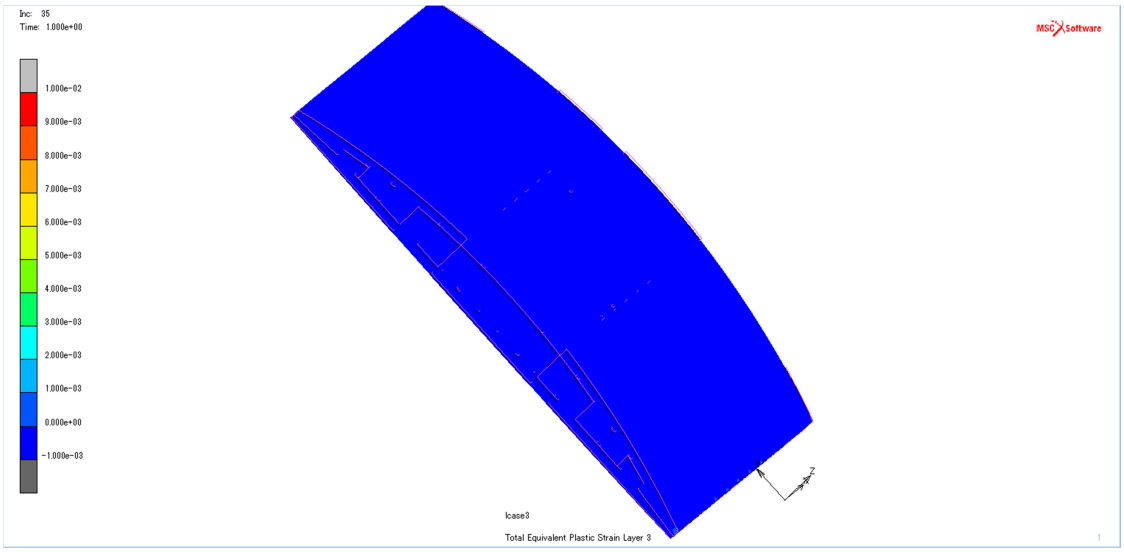

Figure 55 Equivalent Plastic strain_Level 1_Case 2

Figure 54 shows the Von Mises stress distribution happening in the structure when subjected to Level 1 – case 2 loading. The Von Mises stresses developed are low in the structure; the maximum range of stresses visible is in between 48 MPa ~ 72 MPa. This stress however is developed due to the boundary effect and hence it could be neglected.

Figure 55 shows the equivalent plastic strain happening in the structure. It is very clear that the structure stays within the elastic range without any plastic deformation. To conclude the structure is safe against L1C2 loads and it follows the design philosophy.

5.6.3 Level I – Case 3

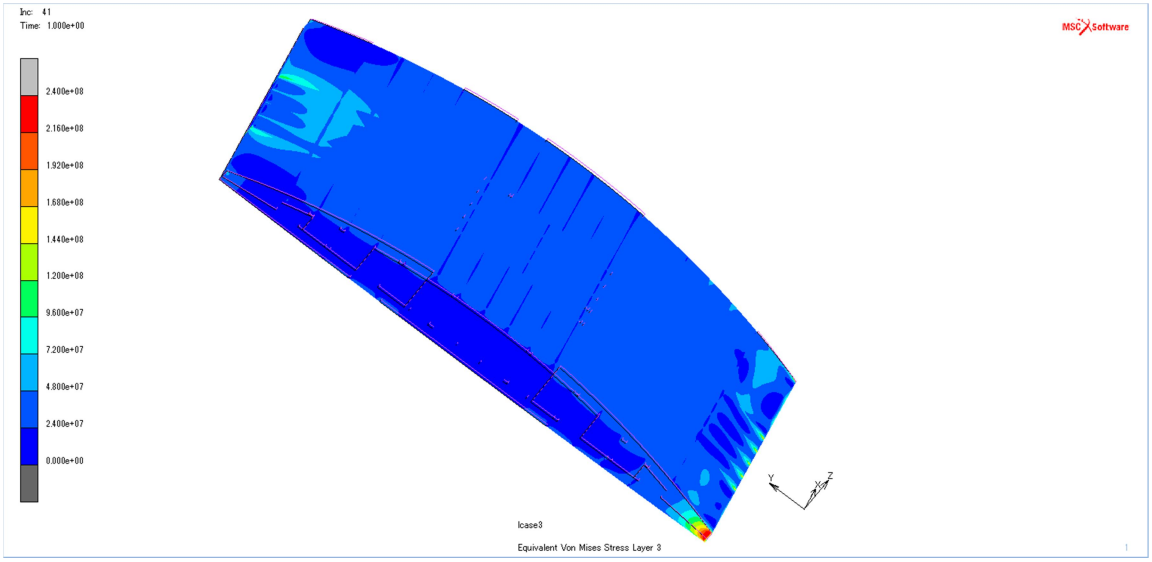

Figure 56 Von Mises stress distribution_Level 1_Case 3

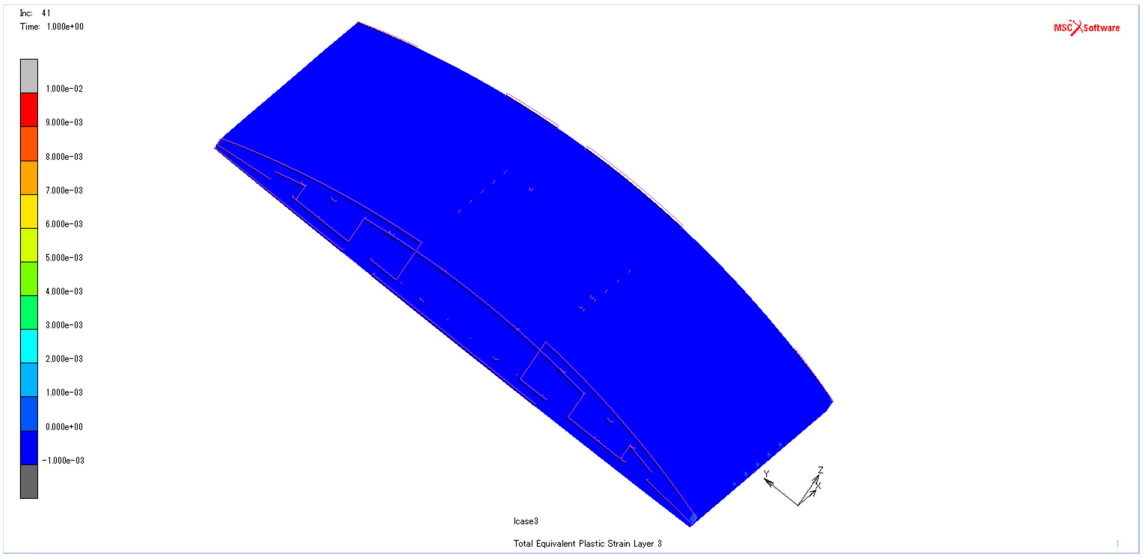

Figure 57 Equivalent Plastic strain_Level 1_Case 3

Figure 56 shows the Von Mises stress distribution happening in the structure when subjected to Level 1 – case 3 loading. The Von Mises stresses developed are low in the structure; the maximum range of stresses visible is in between 48 MPa ~ 72 MPa. This stress however is developed due to the boundary effect and hence it could be neglected.

Figure 57 shows the equivalent plastic strain happening in the structure. It is very clear that the structure stays within the elastic range without any plastic deformation. To conclude the structure is safe against L1C3 loads and it follows the design philosophy.

5.6.4 Level II – Case 1

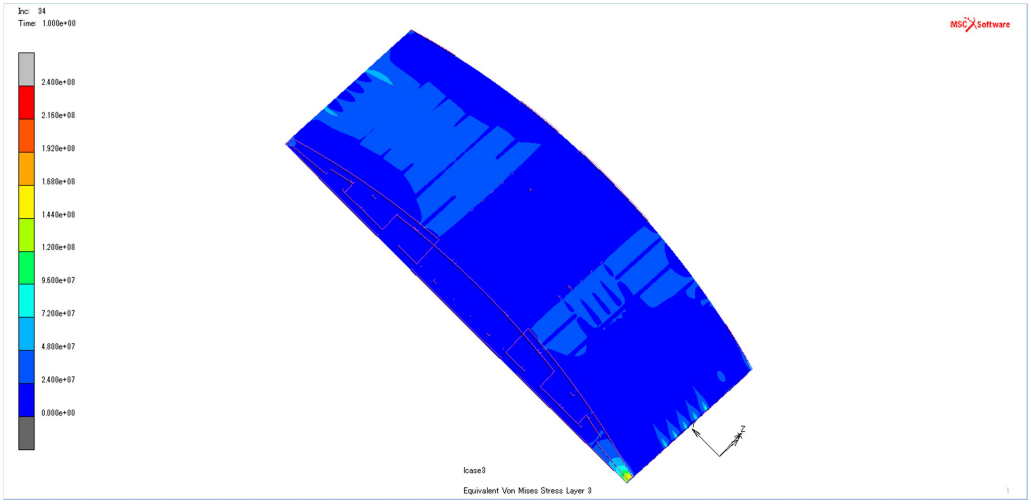

Figure 58 Von Mises stress distribution_Level 2_Case 1

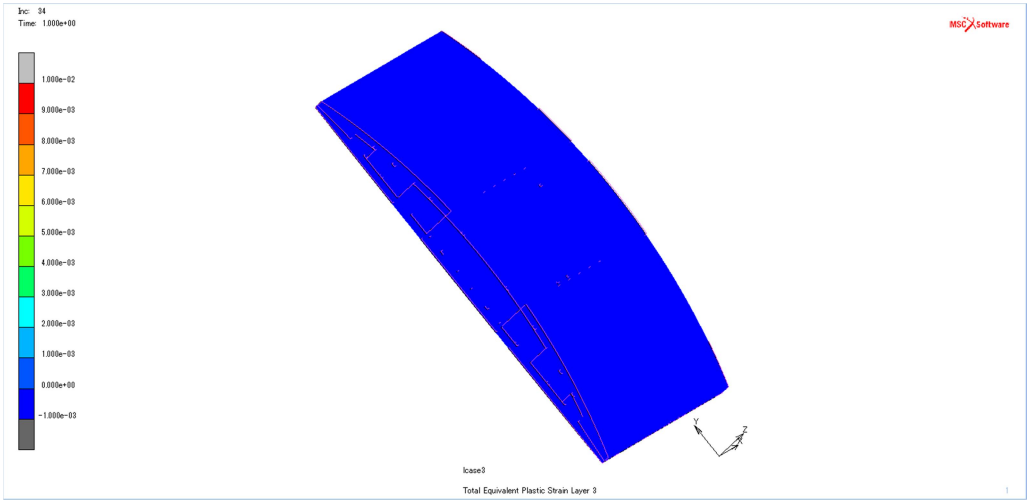

Figure 59 Equivalent Plastic strain_Level 2_Case 1

Figure 58 shows the Von Mises stress distribution happening in the structure when subjected to Level 2 – case 1 loading. The Von Mises stresses developed are comparatively low in the structure; the yield stress being 240 MPa, the maximum range of stress visible is in the range of 24 MPa~ 48 MPa in some parts of the structure.

Figure 59 shows the equivalent plastic strain happening in the structure. As per the design philosophy the structure can deform plastically when subjected to Level II loads, but from the results above it can be noticed that the structure still remains in the elastic region for this loading case. The objective is satisfied however, showing the structure safety against L2C1 loads.

5.6.5 Level II – Case 2

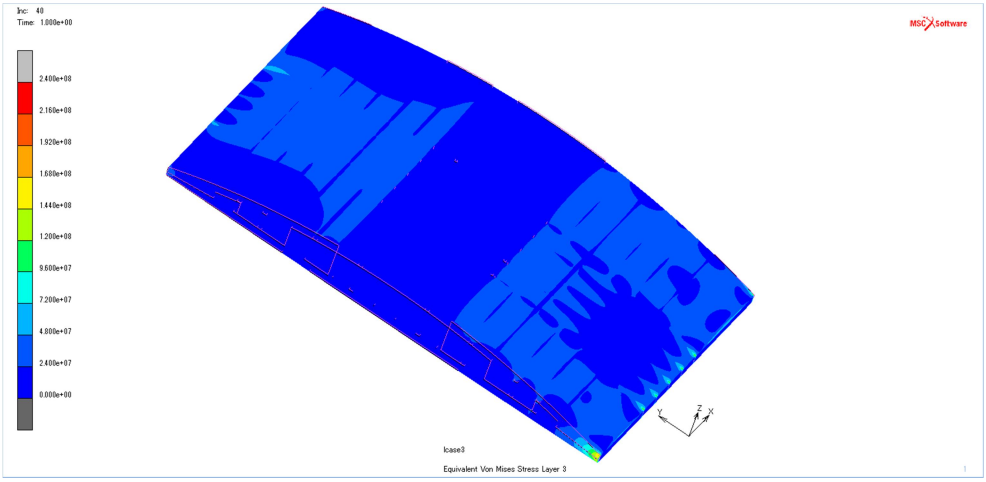

Figure 60 Von Mises stress distribution_Level 2_Case 2

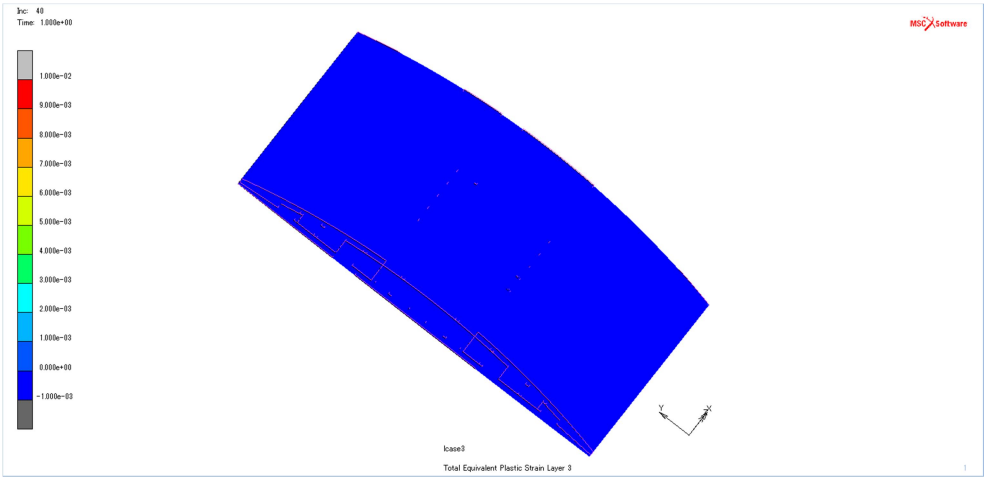

Figure 61 Equivalent Plastic strain_Level 2_Case 2

Figure 60 shows the Von Mises stress distribution happening in the structure when subjected to Level 2 – case 2 loading. The Von Mises stresses developed are comparatively low in the structure; the yield stress being 240 MPa, the maximum range of stress visible is in the range of 24 MPa~ 48 MPa in some parts of the structure.

Figure 61 shows the equivalent plastic strain happening in the structure. As per the design philosophy the structure can deform plastically when subjected to Level II loads, but from the results above it can be noticed that the structure still remains in the elastic region for this loading case. The objective is satisfied however, showing the structure safety against L2C2 loads.

5.6.6 Level II – Case 3

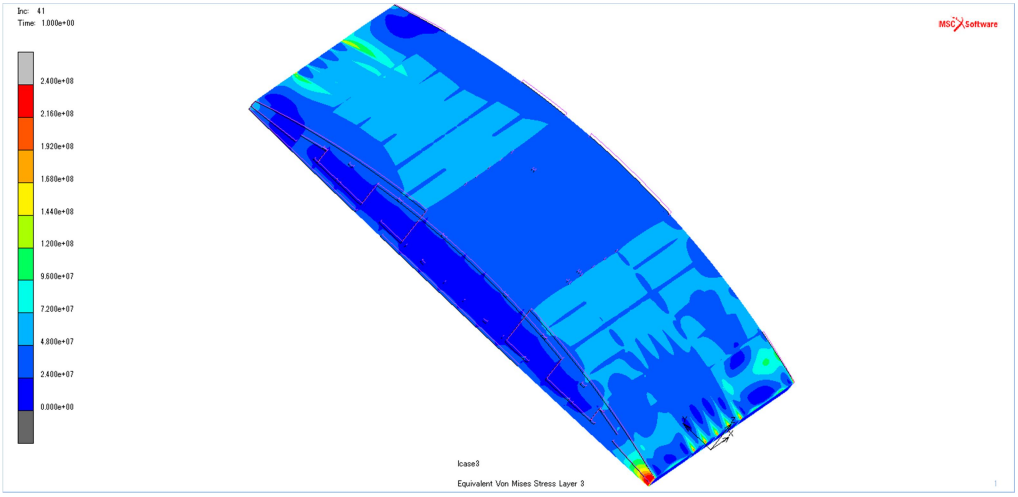

Figure 62 Von Mises stress distribution_Level 2_Case 3

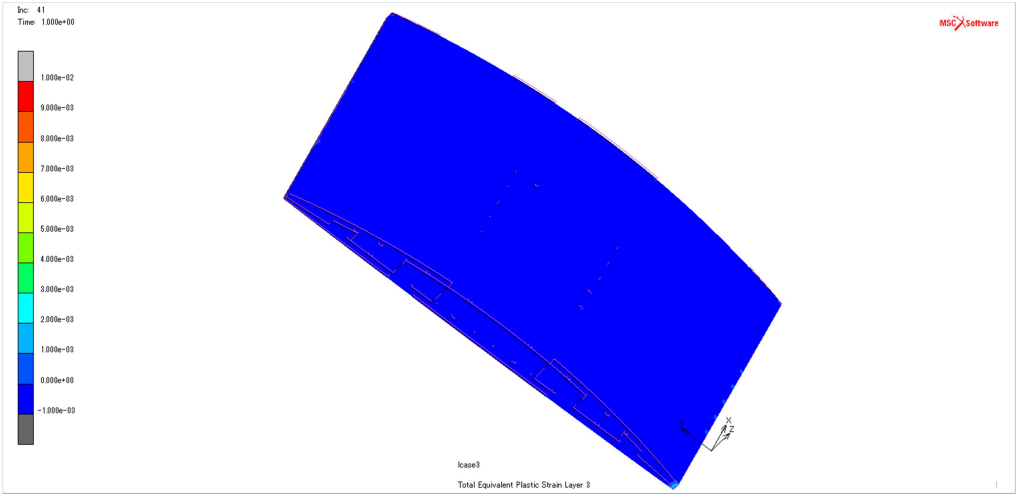

Figure 63 Equivalent Plastic strain_Level 2_Case 3

Figure 62 shows the Von Mises stress distribution happening in the structure when subjected to Level 2 – case 3 loading. The Von Mises stresses developed are comparatively low in the structure; the yield stress being 240 MPa, the maximum range of stress visible is in the range of 48 MPa∼ 72 MPa in some parts of the structure.

Figure 63 shows the equivalent plastic strain happening in the structure. As per the design philosophy the structure can deform plastically when subjected to Level II loads, but from the results above it can be noticed that the structure still remains in the elastic region for this loading case. The objective is satisfied however, showing the structure safety against L2C3 loads.

5.7 Results summary

Table 13 Results summary for L1/L2 loads

Tsunami type	Structure behaviour		
	Safety	Elastic deformation	Plastic deformation
L1C1	Yes	Yes	No
L1C2	Yes	Yes	No
L1C3	Yes	Yes	No
L2C1	Yes	Yes	No
L2C2	Yes	Yes	No
L2C3	Yes	Yes	No

6. ULTIMATE STRENGTH EVALUATION OF THE STRUCTURE

The evaluation of Ultimate strength of the structure is carried out using extreme Tsunami loads. For this the loading case L2C3 is kept as the base loading and it is incremented proportionally. Each proportional incremental case of loading is applied on to the structure and nonlinear static analysis is performed as an iterative process, until the structure collapses.

- Base Load for Ultimate strength evaluation (Level II – Case 3)

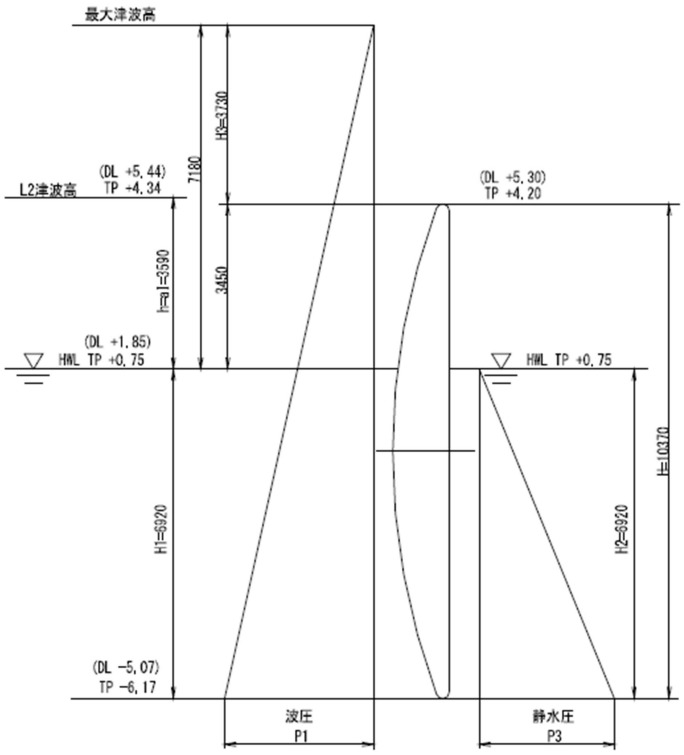

Figure 64 L2C3 Loading

P1 = 149.531 kN/m^2, P2 = 39.557/m^2, P3 = 62.903 kN/m^2

6.1 Loading

Table 14 Loading-Ultimate strength evaluation

Case	Pressure(kN/m2)			
	P1	P2	P3	Belt
1	299.06	79.11	125.81	6358.49
2	448.59	118.67	188.71	9537.73
3	598.12	158.23	251.61	12716.98

6.2 Results overview

6.2.1 Case 1

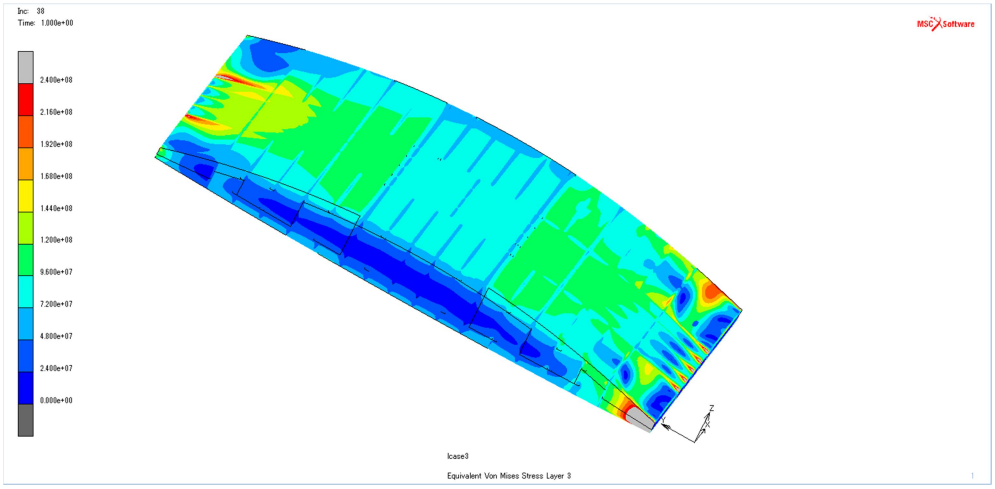

Figure 65 Von Mises stress distribution

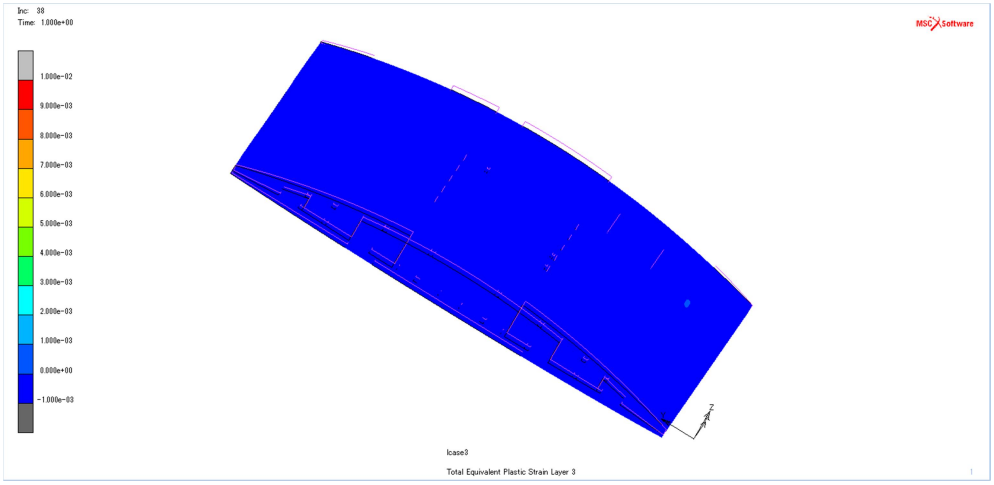

Figure 66 Equivalent plastic strain

Figure 65 shows the Von Mises stress distribution happening in the structure when subjected to case 1 loading for evaluation of Ultimate strength of the structure. The maximum Von Mises stresses developed are in the range of 120 MPa∼ 144 MPa in some parts of the structure; the yield strength of the material being 240 MPa the stresses developed are in the allowable range.

Figure 66 shows the equivalent plastic strain happening in the structure. As per the design philosophy the structure can deform plastically when subjected to Level II loads, but from the results above it can be noticed that the structure still remains in the elastic region for this loading case. The structure is safe against the case 1 loading.

6.2.2 Case 2

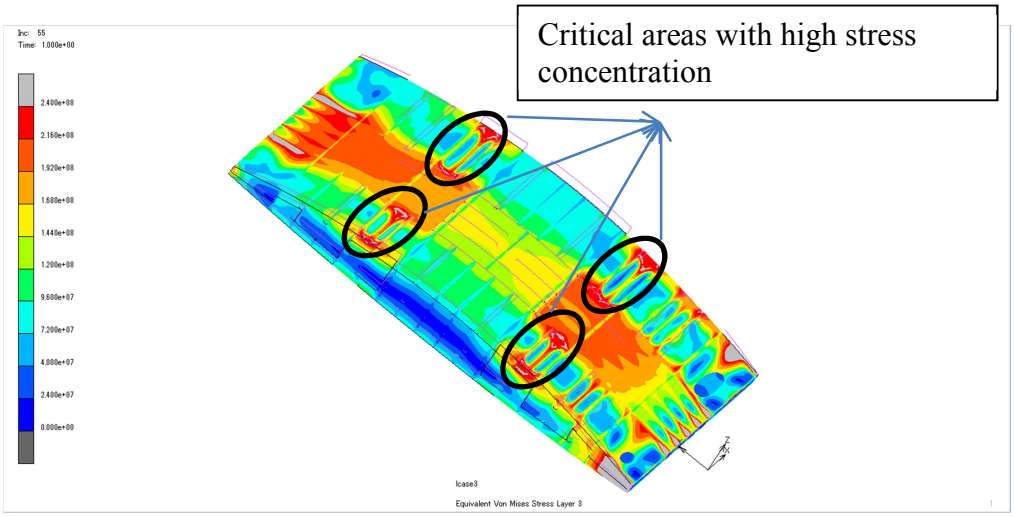

Figure 67 Von Mises stress distribution

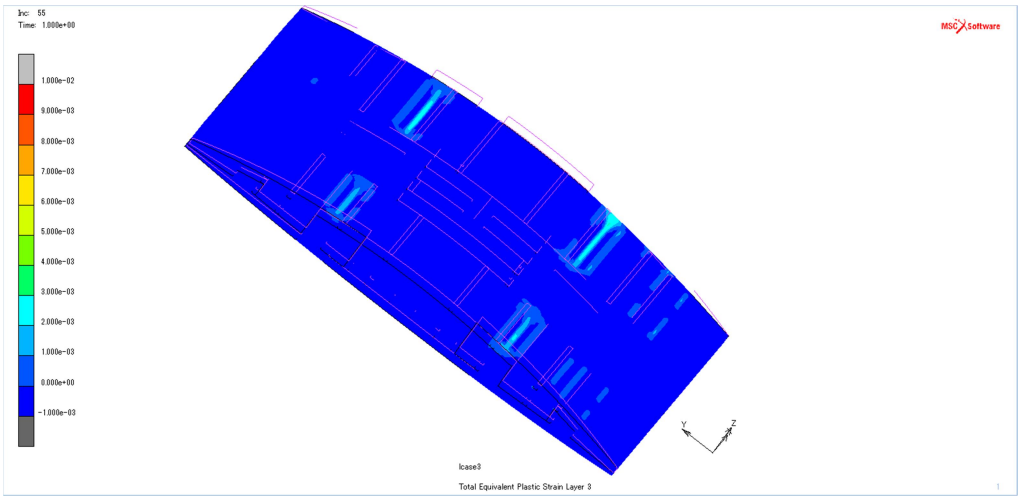

Figure 68 Equivalent plastic strain

Figure 67 shows the Von Mises stress distribution happening in the structure when subjected to case 2 loading for evaluation of Ultimate strength of the structure. The maximum Von Mises stresses developed are in the range of 216 MPa∼ 240 MPa and even more in some parts of the structure; the yield strength of the material being 240 MPa the stresses developed are high. The highlighted portions in Figure 67 are the critical areas in the structure, where the stress concentrations are high.

Figure 68 shows the equivalent plastic strain happening in the structure. As per the design philosophy the structure can deform plastically when subjected to Level II loads. From the results above it can be noticed that some parts in the structure undergoes plastic deformation. Still the structure is safe against the case 2 loading.

6.2.3 Case 3

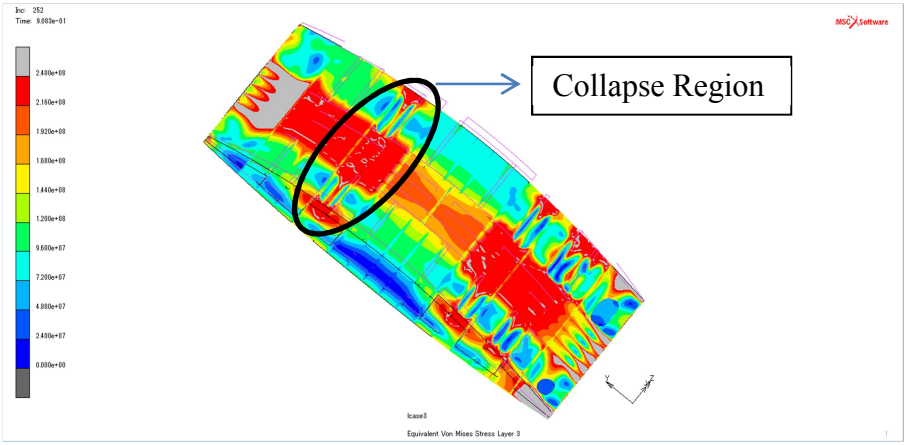

Figure 69 Von Mises stress distribution

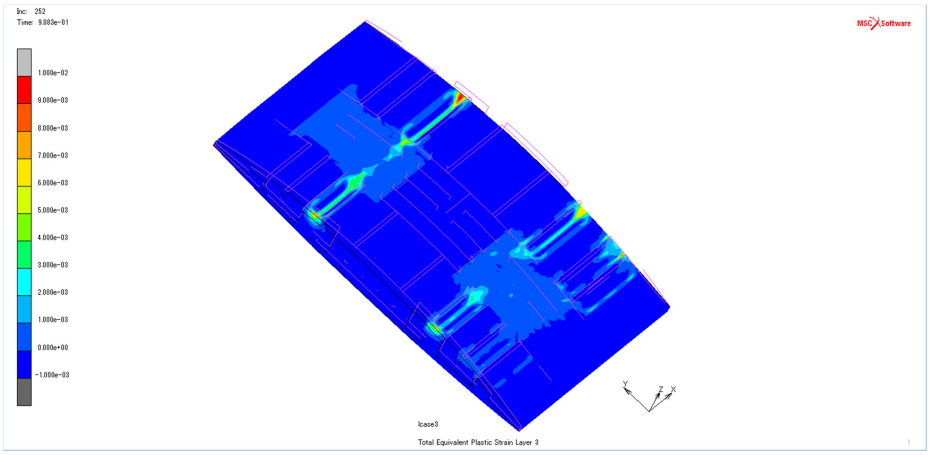

Figure 70 Equivalent plastic strain

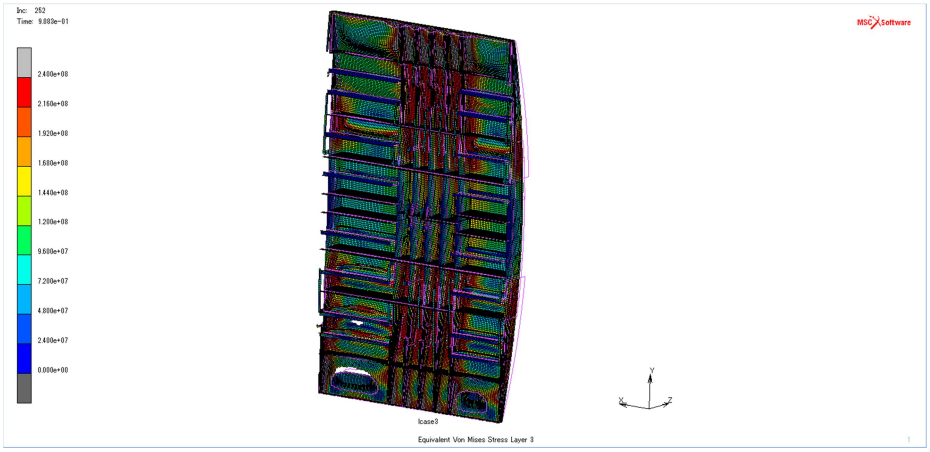

Figure 71 Inside view of structures

For case 3 extreme loading, at around 90% of the loads the structure undergoes ultimate collapse. The analysis stops at this point and the de-loading starts.

Figure 69 represents the Von Mises stress distribution in the structure just before the collapse happens. It is evident from the figures that the stress concentrations are very high, maximum stresses going beyond the yield strength of the material. The collapse is happening at the highlighted region in figure 69.

Figure 70 shows the plastic deformation happening in the critical areas of the structure. Figure 71 shows the structural behaviour of the inside structures at the time of collapse.

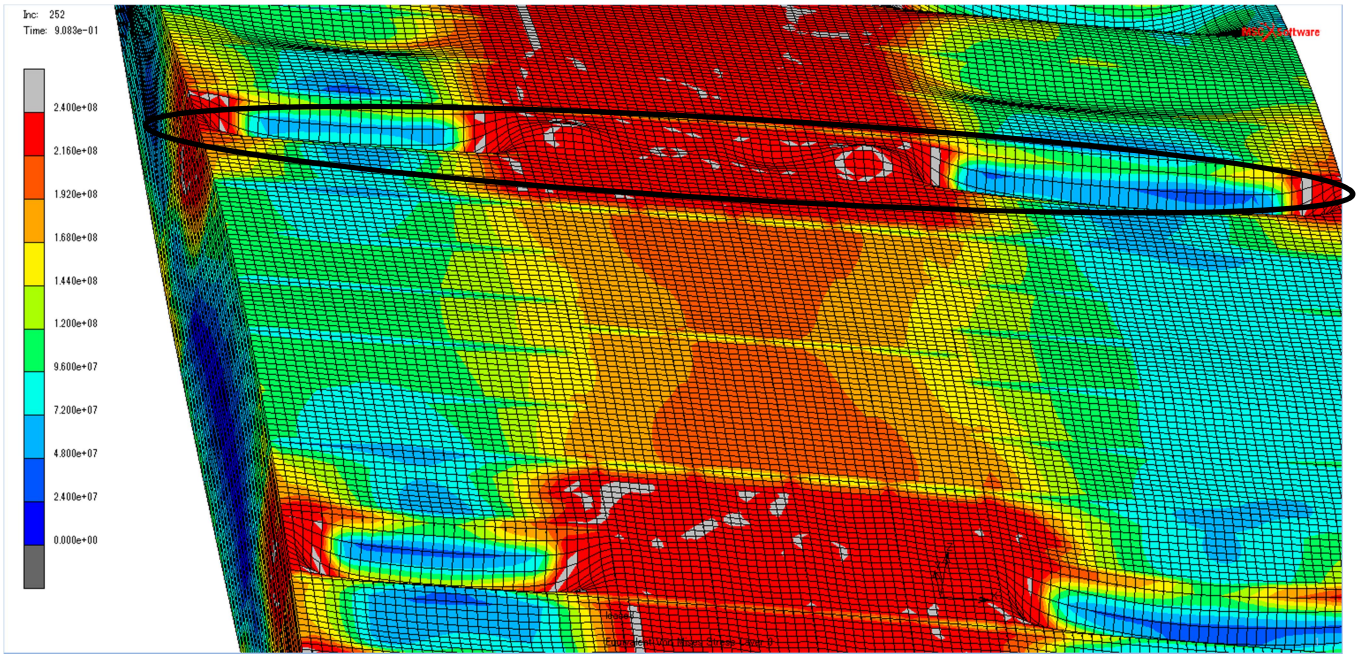

Figure 72 Closer view at the collapse region

Having a closer look of the collapse region (highlighted region) in Figure 72, it can be noticed that the plates are having the buckling tendency.

6.3 Explanation for the collapse behaviour of the structure

The sea gate is simply supported at both the upper and the lower end and receives the lateral pressure as shown in Figures 41 to 46. While the plate is locally subjected to lateral pressure, it is compressed in the y direction due to global bending. Figure 73 shows the bending moment distribution in the structure, calculated manually when subjected to lateral pressure. Although the maximum bending moment is generated around the centre of the sea gate, maximum bending stress takes place around adjacent plates of the centre plate where thinner plate is used.

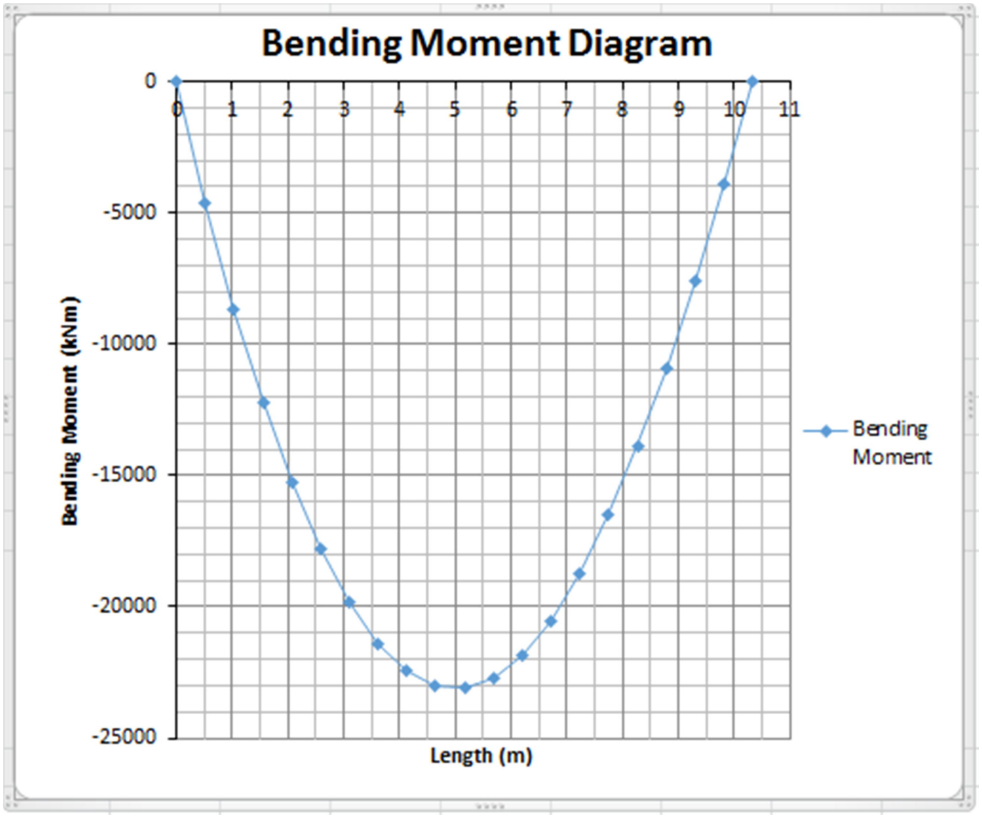

Figure 73 Bending moment distribution in the structure due to the lateral pressure

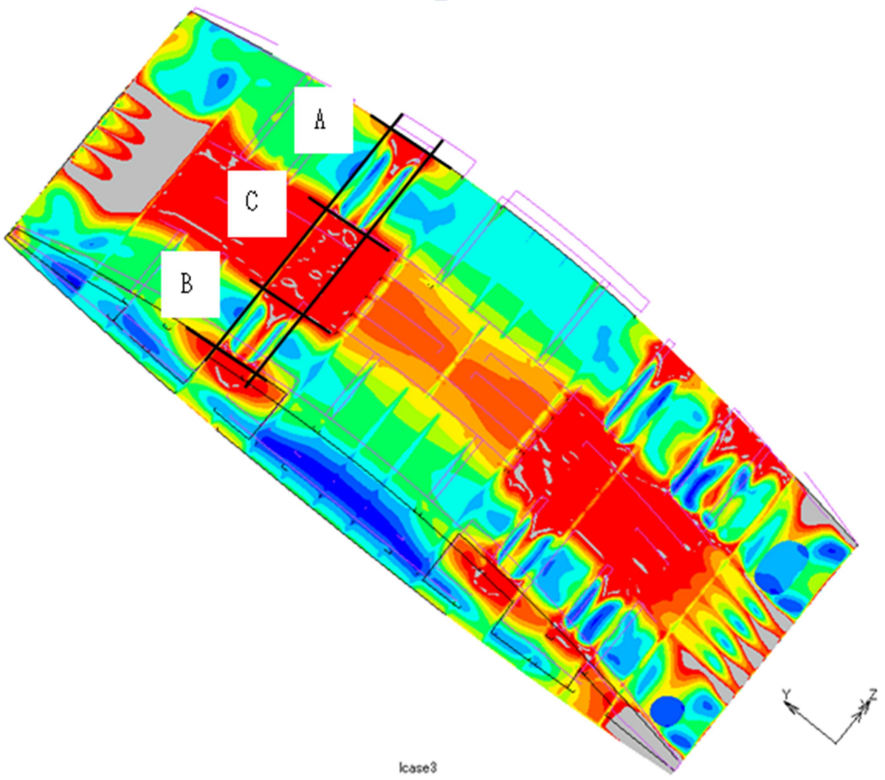

Figure 74 Collapse beahaviour of the structure

Firstly, the plate A in Fig. 74 which has the largest aspect ratio is collapsed with buckling due to the combined compression and the lateral pressure. Subsequently, the plate B is collapsed in the same manner. Since the effective width of the plates A and B is significantly decreased by the buckling, the plate C which are densely supported by vertical girders carries most of the compression from the global bending. It means that the compressive stress is redistributed from A and B to C. Lastly, the plate C is collapsed due to the large compression, and the sea gate attains its ultimate strength.

6.4 Results summary

Table 15 Collapse analysis summary

Collapse evaluation case	Structure behaviour		
	Elastic deformation	Plastic deformation	Collapse
Case 1	Yes	No	No
Case 2	Yes	Yes	No
Case 3	Yes	Yes	Yes

7. CONCLUSIONS AND RECOMMENDATIONS FOR FUTURE WORK

7.1 Conclusion

The research objective of the thesis was to analyse the structural behaviour of the Sea Gate structure against Level I and Level II Tsunamis followed by the Ultimate strength evaluation for the same. With the available data/drawings from the designer of the Sea Gate - Marsima Aqua systems, a relevant symmetric section was considered. It was then modelled and meshed with MSC Patran. The meshed model was then exported to FEA solver MSC MARC for performing the nonlinear analysis against different loading cases.

The nonlinear analysis was performed considering relevant boundary conditions. Six cases were studied; three cases each for Level I and Level II Tsunamis. For Level I tsunamis, the results go in line with the design philosophy; the structure undergoes only elastic deformation and the structure is safe totally against each load cases. For Level II tsunamis the structure can undergo plastic deformation as per design philosophy. However from the results it is clear that the structure still remains in the elastic deformation region, which is OK. The structural safety against both L1 and L2 loads are shown fulfilling the research objective.

The Ultimate collapse strength of the structure was analysed using some extreme Tsunami loads that are derived from the Level II-Case 3 loading. At around 90 % of the case 3 loading considered for the ultimate strength evaluation the structure collapse happens. From the results available it is noticed that the reason for the ultimate collapse of the structure is the combined effect of buckling with yielding of the plate.

7.2 Recommendations for future works

- In this research, the belt associated with the sea gate structure is not modelled along with the structure in MSC Patran for performing the nonlinear analysis using MSC MARC. Instead the effect of the belt is calculated manually and applied as pressure vertically on to the structure for performing the analysis. However it is recommended to model the belt along with the structure and exported to the FE solver for the analysis part and the results needs to be compared.
- The critical area during the collapse analysis of the structure could be modelled separately, with appropriate boundary conditions. It could be analysed separately for the better understanding of the collapse nature.
- The design formula for the structure can be implemented which accounts for the global bending, local bending and buckling together.

8. ACKNOWLEDGEMENTS

This thesis was developed in the frame of the European Master Course in “Integrated Advanced Ship Design” named “EMSHIP” for “European Education in Advanced Ship Design”, Ref.: 159652-1-2009-1-BE-ERA MUNDUS-EMMC.

First of all, I would like to express my deep gratitude to my thesis supervisors Prof. Iijima Kazuhiro and Prof. Akira Tatsumi of Osaka University, Japan for their constant support at every moment of my tenure there for my internship there. I have learned many things from them on day to day basis and they steered me in the right direction whenever they thought I needed it. Also, I would like to thank Prof. Maciej Taczala, my supervisor in West Pomeranian University of Technology, Szczecin for his valuable support and guidance during my internship period and the following days of mine at the West Pomeranian University of Technology.

I would also like to convey my very profound gratitude to Prof. Philippe Rigo, who gave me an opportunity to be a part of the EMSHIP program.

Also, I would like to acknowledge Ms. Htoo Ko, a researcher at the Osaka University for providing me with guidance and help on various tools to carry out my thesis work. Without her passionate participation and input, the work should not have been conducted successfully.

Also, I would like to thank Mr Joseph Praful, my batch mate from current course for his valuable support.

Finally, I must express my very profound gratitude to my parents for providing me with unfailing support and continuous encouragement throughout my years of study.

9. REFERENCES

1. Characteristics of the 2011 Tohoku Tsunami and introduction of two level Tsunamis for Tsunami disaster mitigation by Shinji Sato
2. https://www.google.com/url?sa=i&source=images&cd=&ved=2ahUKEwiQ5Oqu8qzfAhWlo4sKHVYtCrAQjRx6BAgBEAQ&url=https%3A%2F%2Fwww.gfdrr.org%2Fsites%2Fdefault%2Ffiles%2Fpublication%2Fknowledge-note-japan-earthquake-1-1.pdf&psig=AOvVaw3DIdi2tzBFbVU0x0uCpkWU&ust=1545343241766723
3. Development of Hydroplane Tsunami Barrier by Prof. Ryuokei Azuma
4. https://www.google.com/maps/place/Nu+Island/@34.167641,134.8035737,4801m/data=!3m2!1e3!4b1!4m5!3m4!1s0x355359a4e95df501:0xe5bf69a7db8932b8!8m2!3d34.16803!4d134.8258747
5. A first course in Finite Elements by Jacob Fish and Ted Belytschco
6. Reference paper to understand nonlinearity by Solidworks
7. http://www2.me.rochester.edu/courses/ME443/NASTRAN/Chpt3RealEigenvalueAnalysis.pdf
8. Estimation of Tsunami force acting on the block armored breakwater due to Soliton fission by Sohei Maruyama, Tomotsuka Takayama, Kenichiro Shimosako, Akihiko Yahiro, Kojiro Suzuki, Toru Aota, Masashi Tanaka2, Akira Matsumoto and Minoru Hanzawa
9. Response to the 2011 Great East Japan Earthquake and Tsunami disaster by Shunichi Koshimura and Nobuo Shuto